THE ASTROPHYSICAL JOURNAL, 432:305–325, 1994 September 1

A SPECTROSCOPIC ANALYSIS OF DAO AND HOT DA WHITE DWARFS: THE IMPLICATIONS OF THE PRESENCE OF HELIUM AND THE NATURE OF DAO STARS

P. BERGERON,[1,2] F. WESEMAEL,[1] A. BEAUCHAMP,[1] M. A. WOOD,[2,3] R. LAMONTAGNE,[1] G. FONTAINE,[1] AND JAMES LIEBERT[4]

Received 1993 December 14; accepted 1994 March 1

ABSTRACT

A comprehensive study of optical spectrophotometry of DAO white dwarfs is presented. A detailed analysis of the He II λ4686 line profiles demonstrates conclusively that the chemical composition in the atmospheres of DAO stars is not stratified, except perhaps in one object (PG 1305−017). On the other hand, line profiles calculated from models with homogeneous compositions are in excellent agreement with the observed profiles. This result indicates that the helium abundance distribution, in the line-forming region, is homogeneous and implies, in turn, that some physical mechanism is competing with gravitational settling to support helium in these layers.

A similar analysis is then carried out for a sample of hot DA stars. In particular, the sensitivity of the atmospheric parameter determination to the presence of unobservable traces of helium in the photosphere is investigated in detail. The results show that, above $\sim$40,000 K, the effective temperatures of DA stars can be overestimated by up to several thousand degrees if spectroscopically invisible traces of helium [N(He)/N(H) $\lesssim 10^{-4}$] are present in their atmospheres. For instance, the optically determined effective temperature of a DA white dwarf with $T_{\rm eff}$ = 60,000 K and N(He)/N(H) = 10^{-4} would be overestimated by $\sim$20,000 K if analyzed with pure hydrogen model atmospheres. In the light of these findings, we present a critical analysis of past and current studies of extreme ultraviolet and X-ray observations of hot DA stars.

A comparison of the atmospheric parameters of the hot DA stars with those of the DAO stars reveals that the presence of helium in most DAO white dwarfs is directly related to their unusually low surface gravities ($\log g \lesssim 7.5$), although several exceptions are found and considered individually. The nature and evolution of DAO white dwarfs is discussed at length. We identify several subclasses of DAO stars, a result which indicates that the DAO spectral class is a rather inhomogeneous collection of objects, with only a few DAO stars in our sample being consistent with post–asymptotic giant branch evolution. We present supporting evidence that the progenitors of most DAO stars are post–extended horizontal branch stars ($M \sim 0.48\ M_{\odot}$) which have evolved directly from the extended horizontal branch to the white dwarf state. Those DAO stars which are members of white dwarf + M dwarf composite systems represent an independent subclass with unique properties. PG 1305−017 is the only DAO star that shows evidence for stratification, while the variable spectrum of PG 1210+533 cannot be reproduced successfully with any of the models explored in this analysis. Finally, we offer observational evidence that the presence of heavy elements is the most plausible explanation for the origin of the so-called Balmer-line problem in DAO stars.

Subject headings: line: formation — stars: abundances — stars: atmospheres — white dwarfs

1. INTRODUCTION

White dwarf stars are remarkable objects in terms of their simple atmospheric composition, either hydrogen- or helium-dominated. Despite this apparent simplicity, studies of the small chemical impurities present in their atmospheres have played a key role in our understanding of the nature and evolution of white dwarf stars. The presence of trace elements provides us with a probe from which the physical properties of white dwarf atmospheres and envelopes can be studied in greater detail.

Hot white dwarfs with pure hydrogen compositions had been expected to be strong sources of soft X-ray and extreme ultraviolet (EUV) radiation (Shipman 1976), but, unexpectedly, the early results from the *Einstein* and *EXOSAT* satellites indicated that most hot DA stars showed a large X-ray flux deficiency (see Vennes et al. 1988, and references therein). This deficiency could be accounted for if small traces of helium, supported by radiation pressure, were to provide the required additional opacity in the soft X-ray spectral window. The detailed calculations of Vennes et al. (1988) showed, however, that the amount of helium supported by radiative acceleration is insufficient to account for the X-ray flux deficiency. Hence, they proposed instead that chemically layered atmospheres, with a thin hydrogen atmosphere floating in diffusive equilibrium on top of a more massive helium envelope, would provide sufficient amounts of helium in the deeper atmospheric regions to absorb the X-ray flux, while still maintaining an almost pure hydrogen superficial layer where most of the

[1] Département de Physique, Université de Montréal, C.P. 6128, Succ. A, Montréal, Québec, Canada, H3C 3J7; bergeron, wesemael, beaucham, lamont, fontaine@astro.umontreal.ca.

[2] Guest observer, Kitt Peak National Observatory, National Optical Astronomy Observatories, operated by the Association of Universities for Research in Astronomy, Inc., under cooperative agreement with the National Science Foundation.

[3] Department of Physics and Space Sciences, Florida Institute of Technology, 150 West University Boulevard, Melbourne, FL 32901-6988; wood@kepler.pss.fit.edu.

[4] Steward Observatory, University of Arizona, Tucson, AZ 85721; liebert@as.arizona.edu.

optical radiation originates. Koester (1989) and Vennes & Fontaine (1992) showed that these stratified models could successfully reproduce most of the *EXOSAT* as well as earlier *Einstein* observations.

Alternatively, Vennes et al. (1989) demonstrated from similar observations that in at least one star, Feige 24, the soft X-ray and EUV flux deficiencies could not be reproduced from stratified configurations, but could be explained, instead, in terms of a host of heavy elements supported by radiative acceleration in the photospheric regions. Vennes (1992) further developed this approach and combined the available optical, ultraviolet, and soft X-ray observations to show that several DA stars were better described with these metal-rich models than with stratified models.

The more complete and more sensitive EUV and soft X-ray all-sky survey by *ROSAT* (Pounds et al. 1993) revealed an even stronger deficiency, with only 119 white dwarf detections out of the 1000–2000 white dwarf sources anticipated (Barstow 1989). The analysis of the white dwarf component of this survey by Barstow et al. (1993a, and references therein) showed that above $T_{\rm eff} \sim 40{,}000$ K, neither homogeneous nor stratified H/He models could, in general, explain the observations. The authors conclude that an additional opacity source, most likely provided by trace elements heavier than helium, would yield a better match to the observations. No such calculations are presented in their analysis, however.

Although stratified models appear physically sounder in view of the results of Vennes et al. (1988), it has never been proved *observationally* that the atmospheres of hot DA white dwarfs have chemically layered rather than homogeneous structures, since the currently available data seem to indicate that heavy elements, instead of helium, provide most of the soft X-ray and EUV absorbing material. We are thus left with no diagnostic to infer the helium abundance distribution throughout the atmosphere, or even to measure if helium is present at all in the atmospheres of hot DA white dwarfs.

White dwarfs with hybrid spectra showing both hydrogen and helium lines may well provide important clues to these problems. In this paper, we focus our attention on the DAO stars, with hydrogen-dominated spectra and weak He II λ4686 features, the prototype of which is HZ 34 (see Wesemael et al. 1993). Wesemael, Green, & Liebert (1985) produced the first comprehensive spectrophotometric and model-atmosphere analysis of DAO white dwarfs using homogeneous composition models, a reasonable assumption at that time. They showed, in particular, that DAO stars have effective temperatures in the range 50,000–70,000 K, with helium abundances of $N({\rm He})/N({\rm H}) \sim 10^{-2}$, typically. The spectroscopic survey of Holberg (1987) significantly enlarged the sample of known DAO stars, and atmospheric parameter determinations of these stars using optical and *IUE* observations, again in terms of homogeneous models, were presented in Holberg et al. (1989).

Fontaine & Wesemael (1987) discussed the possibility that a large fraction of all white dwarfs may have evolved from helium-rich PG 1159 stars. New observational evidence (see, e.g., Napiwotzki & Schönberner 1993b, Liebert, Bergeron, & Tweedy 1994) indicates, however, that many central stars of old planetary nebulae already have *hydrogen-rich* atmospheres. Nevertheless, it remains possible that a fraction of the DA star population may have evolved from PG 1159–like stars: As these stars cool down, residual hydrogen thoroughly mixed in the helium-rich envelope eventually diffuses upward, and a thicker hydrogen atmosphere is gradually being built up at the surface, transforming a helium-rich atmosphere into a hydrogen-rich atmosphere. In this context, DAO stars could be interpreted as intermediate objects undergoing a spectroscopic metamorphosis. If this interpretation is correct, the helium abundance distribution in such objects is given by the diffusive equilibrium abundance profile, and the atmospheres of DAO stars should consequently have chemically stratified atmospheres. Vennes et al. (1988) even demonstrated from theoretical considerations that stratified configurations are the only viable explanation (with the possible exception of stellar winds) for the presence of helium in DAO stars.

No thorough detailed spectroscopic analysis of DAO stars has been produced yet to confront the predictions of homogeneous and stratified models with observed line profiles. Isolated analyses of the DAO stars LS V+46 21 by Napiwotzki & Schönberner (1993b) and Feige 55 by Bergeron et al. (1993) indicate, most unexpectedly, that model spectra calculated from homogeneous composition models yield excellent fits to the observed He II λ4686 line profile, while the profiles calculated from stratified models are predicted to be too broad and shallow. These puzzling results have led us to investigate a larger sample of DAO stars to understand better the helium abundance distribution in these objects.

Also of interest is the "Balmer-line problem" discussed by Napiwotzki & Rauch (1994, and references therein). It is found that the observed Balmer-line profiles of many DAO central stars of old planetary nebulae cannot be fit simultaneously with a single model spectrum, and discrepant temperatures are derived if the lines are considered individually. A discrepancy of a similar nature was encountered in the DAO star Feige 55, as reported by Lamontagne et al. (1993) and Bergeron et al. (1993). Napiwotzki & Rauch reviewed all the explanations offered up to now of this phenomenon, all of which have failed so far (see below, however). After exploring yet another effect, namely, the effect of ion dynamics on the Balmer-line profiles, they conclude that the Balmer-line problem remains unresolved. The systematic study of a large sample of DAO stars undertaken here should therefore shed more light on this puzzle.

In order to provide a global picture of the atmospheric properties of DAO stars with respect to other white dwarf stars, it was deemed necessary to include as well in our study a line profile analysis of DA stars in the same range of effective temperatures. In particular, we explore below the effect of the presence of small traces of helium on the atmospheric parameter determinations of hot DA stars, an effect which has been largely overlooked in previous analyses.

The observing material and theoretical models which represent the backbone of our analysis are presented in §§ 2 and 3, respectively. Our sample of DAO stars is then analyzed in § 4, while § 5 is devoted to the analysis of the hot DA stars. The results are then combined in § 6, where the nature of DAO stars is discussed at length. We then offer new insight to the Balmer-line problem in § 7 and summarize our conclusions in § 8.

2. SPECTROSCOPIC OBSERVATIONS

Most of the spectroscopic observations used in this analysis were obtained as part of a program aimed at constraining the mass of the hydrogen layer in DA white dwarfs (Wood & Bergeron 1994). A sample of 37 stars of spectral type DA1 was selected from the catalog of spectroscopically identified white

dwarfs of McCook & Sion (1987). No attempt was made to obtain a complete magnitude-limited sample, although objects with a wide range of apparent visual magnitudes were selected to minimize biases such as those discussed in Bergeron, Saffer, & Liebert (1992, hereafter BSL). We also included in our sample PG 1234+482, originally classified as a subdwarf B star in the Palomar-Green catalog, but later reclassified DA1 by Jordan, Heber, & Weidemann (1991) after its rediscovery in the Hamburg-Schmidt Survey (HS 1234+4811).

The spectroscopic observations for this sample were carried out during 1992 March 24–26 UT at the Kitt Peak National Observatory 2.1 m telescope, using the Gold Spectrograph CCD Camera equipped with a FORD 3K chip. The 4″.5 slit together with the 600 line mm^{-1} grating blazed at λ4400 in first order provided a spectral coverage of $\lambda\lambda$3650–5140 at an intermediate resolution of $\sim$8 Å FWHM. The signal-to-noise ratio is above 80 in most cases. Four objects (PG 1121+145, HZ 39, Feige 91, and PG 1450+432) turned out to be sdB stars, the analysis of which will be reported elsewhere. Ton 320 (PG 0823+316), Ton 353 (PG 0846+249), and PG 1305−017 were classified DA1 in McCook & Sion but were later reclassified DAO by Holberg (1987), while PG 0834+501 and LB 2 (PG 1214+267) are newly discovered members of the DAO spectral class.

Independently, we also obtained spectra of other DAO stars of particular interest, some of which have already been analyzed elsewhere but which are reanalyzed here for completeness. All objects have been observed using the setup described in BSL, or otherwise stated in the references given below. LS V+46 21, the central star of the planetary nebula S216, has been analyzed by Tweedy & Napiwotzki (1992); we obtained two separate observations of this star and performed an independent analysis. HZ 34, PG 1210+533, and PG 0134+181 have been observed as part of a project to redetermine the luminosity function of DA white dwarfs. The last object has been reported by Holberg (1987) and Holberg et al. (1989) *not* to show the He II λ4686 or the He II λ1640 lines, but our spectrum (Fig. 1) clearly shows the former feature, and the object is therefore a DAO star. GD 561 was classified DA2 in the McCook & Sion catalog but was later reclassified DAO by BSL; Napiwotzki & Schönberner (1993a) argue that GD 561 is the central star of the planetary nebula S174. Feige 55 (PG 1202+608, GD 314) was classified sdB both in the early list of Greenstein & Sargent (1974) and later in the Palomar-Green catalog (Green, Schmidt, & Liebert 1986). In the McCook & Sion catalog (see the reference to Szathmary 1972), however, it is listed as a white dwarf! Independent observations by us and Saffer (1992, private communication), as part of spectroscopic programs aimed at determining the atmospheric parameters of sdB stars, confirmed the membership of Feige 55 to the DAO spectral class. A detailed analysis of this object has been presented by Bergeron et al. (1993). The analyses of RE 1016−053 and PG 1413+015 have been carried out by Tweedy et al. (1993) and Fulbright et al. (1993), respectively, and are repeated here for completeness. The spectrum of RE 2013+400 is displayed in Barstow et al. (1993c) and has been kindly provided to us by R. W. Tweedy. Although we present only a summary of the atmospheric parameter determination for this object, a full analysis of the available data will be presented elsewhere (Tweedy et al. 1994). Finally, we exclude PG 0950+139 (the DAO central star of the planetary nebula EGB 6) from our analysis since the Balmer lines are heavily contaminated, at the medium resolution employed here, by emission lines from the surrounding nebula.

The samples of DAO and DA1 stars are displayed in Figures 1 and 2, respectively. PG 1527+091, LS V+46 21, and Feige 55 have multiple observations which can be used to obtain an external check of our atmospheric parameter determination.

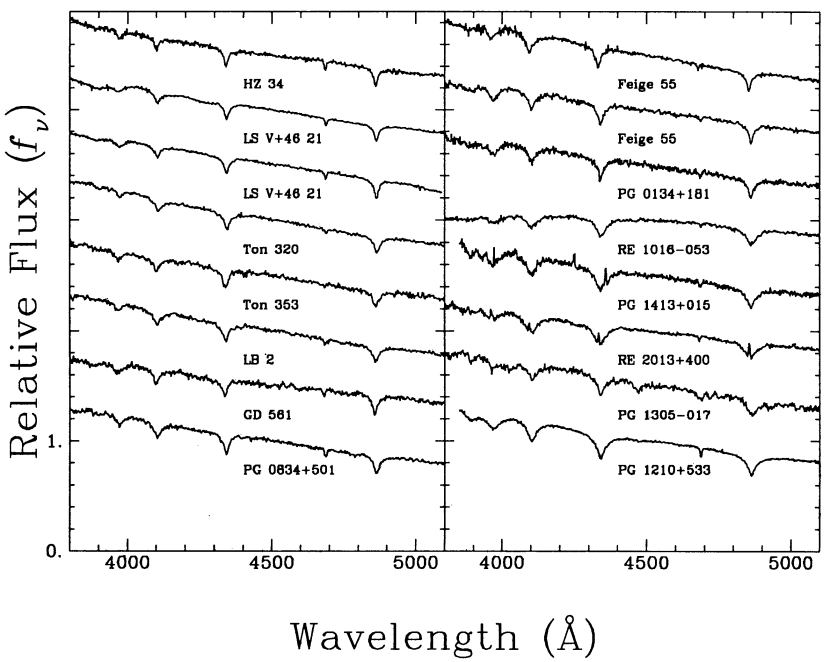

FIG. 1.—Optical spectra for the sample of 14 DAO stars as defined in the text. The spectra are normalized to unity at 4500 Å and are shifted vertically by 0.5 for clarity. The effective temperature decreases from upper left to bottom right, approximately. The spectral resolution of this sample varies from 6 to 8 Å (FWHM). For LS V+46 21 and Feige 55, two spectra were secured and are shown.

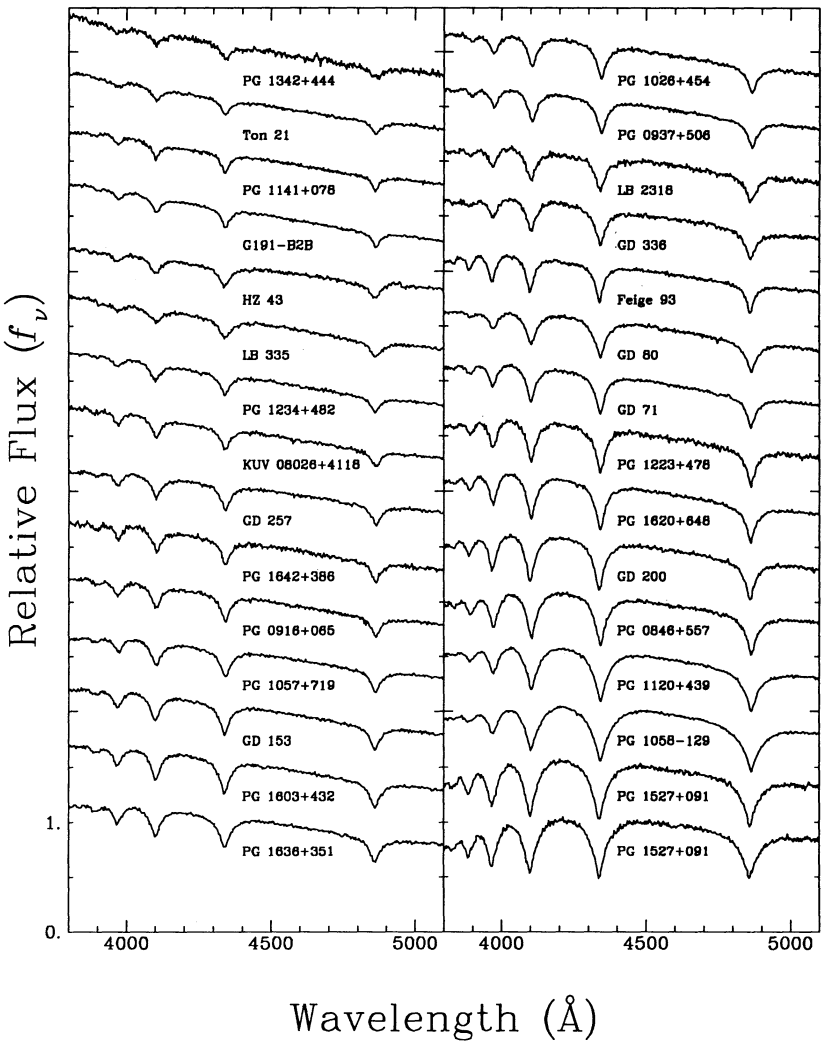

FIG. 2.—Optical spectra for the sample of DA1 stars of Wood & Bergeron (1994). As in Fig. 1., the spectra are normalized to unity at 4500 Å and are shifted vertically by 0.5 for clarity. The effective temperature decreases from upper left to bottom right. The spectral resolution of this sample is ~8 Å (FWHM). PG 1527+091 has been observed twice, and both spectra are displayed.

As can readily be seen from Figure 2, the sample of DA1 stars covers a wide range of effective temperatures. The fluxing of RE 1016−053, as discussed by Tweedy et al. (1993), suffers from the fact that the spectrograph was not rotated along the atmospheric dispersion, in order to avoid contamination from the adjacent M dwarf 5″ to the north. Note also the presence of strong He I lines in the DAO star PG 1305−017, and of much weaker ones in PG 1210+533.

Below, we also use archival *IUE* observations to verify the internal consistency of our atmospheric parameter determinations. All images were reprocessed using the *IUE* Regional Data Analysis Facility (RDAF) at GSFC over the Internet. A Gaussian slit extraction technique was applied to the original two-dimensional low-dispersion spatially resolved line-by-line files. Absolute fluxes for both SWP and LWR images were based on the new calibration of Finley, Basri, & Bowyer (1990); LWP spectra were scaled with the flux calibration from Cassatella, Lloyd, & Gonzalez Riestra (1987). The time-dependent degradation was corrected following the prescription of Bohlin & Grillmair (1988) for SWP and LWR images, and Teays & Garhart (1990) for LWP images. For a given star, when several images were available for the same spectral region, they were averaged after all the flux corrections were accounted for.

3. MODEL ATMOSPHERES AND SYNTHETIC SPECTRA

We have analyzed all stars with models calculated assuming both homogeneous and stratified chemical compositions. The homogeneous model atmospheres are similar to those described in Wesemael et al. (1980), while the stratified configurations have been calculated using the formalism discussed at length in Jordan & Koester (1986) and Vennes & Fontaine (1992). The atmospheric parameters of the homogeneous models cover a range of $T_{\rm eff}$ = 20,000 (5000) 100,000 K (where the quantity in parentheses indicates the step size), log g = 6.5 (0.5) 8.5, and log $y \equiv \log N({\rm He})/N({\rm H}) = -5.0$ (1.0) 0.0. Pure hydrogen models were calculated, as well. For the stratified models, we define the quantity $Q \equiv 3 \log g + 2 \log q_{\rm H}$, where $\log q_{\rm H} \equiv \log M_{\rm H}/M_*$. This definition allows spectra for a given value of Q to look relatively similar (with respect to the strength of the helium lines) in the (log g, log $q_{\rm H}$)-plane. Therefore, for each assumed value of log g, we consider a different

range of log q_H. Models calculated with $Q = -10.0$ (1.0) -6.0 [i.e., log $q_H = -17.0$ (0.5) -15.0 at log $g = 8.0$] embrace the entire spectral properties of the DAO stars analyzed here.

The emergent spectra have been calculated following Bergeron, Wesemael, & Fontaine (1991; see also BSL and Bergeron 1993), where our treatment of the hydrogen line profiles is described at length. The He II λ1640 and λ4686 line profiles have been interpolated from the tables of Schöning & Butler (1989). These are the only He II lines detectable in the DAO observations discussed below. The He I lines, visible in the coolest DAO stars of our sample, have been treated as Voigt profiles with the Stark broadening parameters of Dimitrijevic & Sahal-Bréchot (1984a, b), with the exception of five transitions whose profiles have been interpolated from the tables of Barnard, Cooper, & Smith (1974; λ4471), Barnard, Cooper, & Smith (1975; λ4921), Barnard & Cooper (1970; λ5016), and Shamey (1969; λ4026, λ4387, and at higher electron densities λ4471 and λ4921). Furthermore, all oscillator strengths have been updated from the results of the Opacity Project (Seaton et al. 1992).

4. THE DAO STARS

4.1. *Analysis with Homogeneous Composition Models*

The atmospheric parameters of each star are determined using our standard procedure of fitting model spectra (convolved with the appropriate instrumental profile) to observed line profiles. Additional details are given in BSL. Here, T_{eff}, log g, as well as N(He)/N(H) are considered free parameters. We exclude from our analysis the two coolest objects, PG 1210+533 and PG 1305−017, which are analyzed separately in § 4.4. The best fits with homogeneous models for our sample of DAO stars are presented in Figure 3, and the atmospheric parameters are summarized in Table 1 in order of decreasing temperature. The uncertainties given in Table 1 represent the *internal* errors of the formal fit as defined in BSL. Since Balmer-line profiles become less sensitive to temperature variations for hotter stars, these internal errors are much larger than those quoted in BSL (100–300 K in T_{eff} and 0.02–0.06 in log g) for their cooler sample of DA stars. Moreover, our analysis includes one additional fitting parameter, N(He)/N(H), and this increases the internal errors even further. The multiple observations of LS V+46 21 and Feige 55 reveal, however, that the atmospheric parameter uncertainties are dominated by the *external* errors originating from independent observations, by data reductions, and, more importantly, by the quality of the flux calibration.

TABLE 1

ATMOSPHERIC PARAMETERS OF DAO STARS OBTAINED FROM HOMOGENEOUS COMPOSITION MODELS

Name	T_{eff}	$\sigma(T_{eff})$	log g	σ(log g)	log y	σ(log y)
HZ 34	79900	3600	6.61	0.20	−1.33	0.24
LS V+46 21	83800	1700	7.17	0.13	−1.71	0.18
LS V+46 21	77300	3400	7.31	0.14	−2.06	0.24
Ton 320	68800	1800	7.68	0.12	−2.74	0.27
Ton 353	66100	2400	7.11	0.19	−2.88	0.52
LB 2	65700	1400	7.67	0.11	−2.51	0.23
GD 561	65300	2000	6.71	0.15	−2.40	0.33
PG 0834+501	60400	1900	7.11	0.12	−2.18	0.23
Feige 55	58300	1500	7.15	0.11	−2.92	0.31
Feige 55	55100	1300	6.96	0.10	−2.91	0.28
PG 0134+181	56400	1500	7.40	0.11	−2.98	0.30
RE 1016−053	56400	1200	7.74	0.07	−3.26	0.22
PG 1413+015	48100	1700	7.69	0.11	−2.57	0.40
RE 2013+400	47800	2400	7.69	0.16	−2.62	0.63

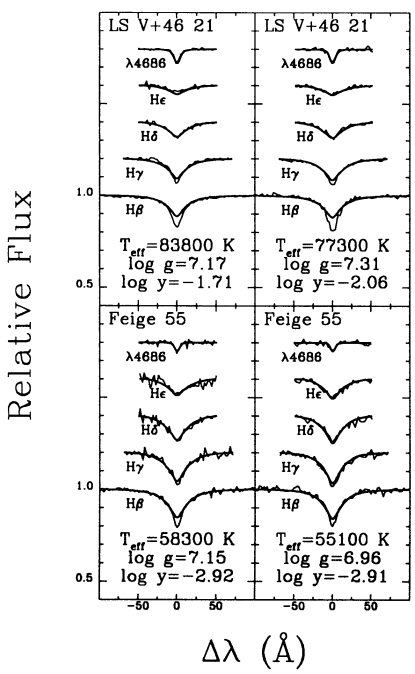

FIG. 3a

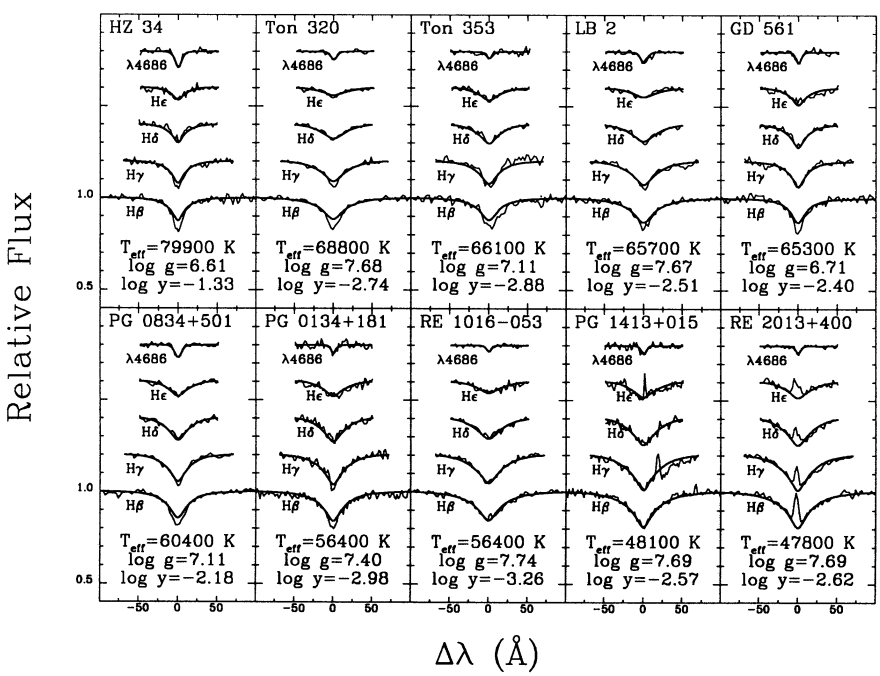

FIG. 3b

FIG. 3.—Fits to the individual Balmer lines and the He II λ4686 line for (*a*) the sample of DAO stars with multiple observations and (*b*) the rest of the DAO stars ordered with decreasing effective temperature. Homogeneous model compositions have been used. In each panel, the lines are normalized to a continuum set to unity and offset vertically by a factor of 0.2.

The fits displayed in Figure 3 present one striking similarity: while excellent fits to the He II λ4686 line profile can be achieved, *it is not possible, for most DAO stars, to achieve a satisfactory fit for all Balmer lines simultaneously from homogeneous models.* This is the well-known Balmer-line problem first pointed out by Napiwotzki (1992) in his analysis of central stars of old planetary nebulae, and briefly discussed in § 1. The results of Figure 3 indicate that this phenomenon is also a characteristic feature of almost all DAO stars that are not central stars of planetary nebulae. Much higher temperatures are generally required to fit the higher lines of the Balmer series as compared to the lower lines. When a "mean" temperature is derived from fitting all line profiles *simultaneously*, the observed profiles of the lower Balmer lines appear deeper than those predicted from the best fit. The only DAO stars in our sample with no such apparent Balmer-line discrepancy are RE 1016−053, PG 1413+015, and possibly RE 2013+400, although in the last object, the cores of the absorption lines are filled in with reprocessed emission by the irradiated hemisphere of the M dwarf companion.

Lamontagne et al. (1993) suggested that the presence of heavy elements observed in the *IUE* images of Feige 55 could hold the key to this problem. This suggestion has been explored more quantitatively by Bergeron et al. (1993) using an approximate LTE calculation of metal-line–blanketed models. Blanketing by iron lines was shown to produce sufficient cooling of the upper atmospheric regions to make the cores of the lower Balmer lines deeper, in much better agreement with the observed line profiles. Bergeron et al. achieved an excellent fit to the line profiles of Feige 55, with an iron abundance of $\log N(\mathrm{Fe})/N(\mathrm{H}) = 10^{-3}$. As mentioned explicitly, however, this iron abundance cannot be taken at face value since the number of iron lines included in their calculations is only a lower limit to the true number of iron lines present in the spectrum. Furthermore, the frequency sampling they used is too coarse, and other sources of metallic opacities have been neglected as well.

More recent calculations by Dreizler & Werner (1993) and Werner & Dreizler (1993), which include a self-consistent non-LTE treatment of iron lines as well as of carbon, nitrogen, and oxygen lines, have shown that the effects of line blanketing by heavy elements are much smaller than predicted by the LTE calculations of Bergeron et al. (1993). However, their calculations have been restricted so far to models with surface gravities much lower ($\log g \lesssim 6.0$) than those encountered in our sample of DAO stars, and additional calculations at higher values of $\log g$ are required before these issues can be settled once and for all. Moreover, we discuss in § 7 circumstantial evidence which strongly suggests that the presence of metallic ions in the photosphere of DAO white dwarfs is indeed the cause of the Balmer-line problem in these stars.

Since it would have been extremely cumbersome to repeat, for each DAO star studied here, an analysis similar to that carried out for Feige 55, we have instead relied upon a different procedure and fit only the wings of each Balmer line, excluding the region ±5 Å from the line cores. For He II λ4686, the entire profile was used. In doing so, we avoided the regions of the spectrum which are formed in the upper atmosphere where the temperature profile is most sensitive to the effects of metal-line blanketing. This approach is shown below to yield results that are satisfactory for the purpose of our analysis. The small differences between the results presented here and those of Bergeron et al. (1993, Fig. 1) with metal-free models are due mainly to this modification in our fitting procedure.

4.2. *Analysis with Chemically Stratified Models*

An analysis identical to that performed above has been carried out with our grid of stratified models. The quality of the fits to the hydrogen line profiles is similar to that obtained from homogeneous models, and those fits are thus not displayed here. In particular, *the use of stratified models did not help to solve the Balmer-line problem*, a result which is consistent with those reported in § 1. The fits to the He II λ4686 line profiles with stratified models, however, are significantly different from our homogeneous fits. We discuss this point further in § 4.3. The results of our atmospheric parameter determination are reported in Table 2.

The effective temperatures derived from stratified models are comparable to those obtained from homogeneous configurations, although significant differences are present for the hottest objects. The largest difference is for HZ 34, where the temperature inferred from stratified models is ∼20,000 K cooler. This last result is somewhat uncertain, however, since the stratified solution is extrapolated in $\log g$ outside our model grid. More typical is the case of LS V+46 21 where the temperature reached from stratified models is 7000–10,000 K cooler than that obtained from homogeneous models. These differences become much smaller at temperatures below ∼65,000 K. The surface gravities obtained from both model sets are also comparable for the cooler DAO stars, but for hotter objects, the $\log g$ values derived from stratified models tend to be lower by about 0.2 dex.

The range of q_{H} values spanned by our sample of DAO stars is larger than that inferred, e.g., by Vennes & Fontaine (1992) who give a limit of $\log q_{\mathrm{H}} \lesssim -15.5$ for typical DAO stars. However, their result is valid for DAO stars at $\log g = 8.0$. For $\log g = 7.0$, a value more appropriate for the DAO stars analyzed here, this limit translates (using our definition of Q) into $\log q_{\mathrm{H}} \lesssim -14.0$, in excellent agreement with the values given in Table 2.

4.3. *Homogeneous or Stratified Compositions?*

As mentioned above, it is not possible to discriminate between homogeneous and stratified composition models solely on the basis of the fits to the Balmer-line profiles. The He II λ4686 line profile, however, turns out to be very sensitive to the helium abundance distribution in the atmosphere, a conclusion reached also by Napiwotzki & Schönberner (1993b). Before making a detailed comparison with the

TABLE 2

ATMOSPHERIC PARAMETERS OF DAO STARS OBTAINED FROM STRATIFIED COMPOSITION MODELS

Name	T_{eff}	$\sigma(T_{\mathrm{eff}})$	$\log g$	$\sigma(\log g)$	$\log q_{\mathrm{H}}$	$\sigma(\log q_{\mathrm{H}})$
HZ 34	60700	2400	6.28	0.17	−13.39	0.27
LS V+46 21	72100	2300	6.97	0.15	−14.24	0.24
LS V+46 21	70500	2100	7.19	0.15	−14.46	0.24
Ton 320	72300	1800	7.68	0.12	−14.98	0.21
Ton 353	67200	2900	7.09	0.19	−14.20	0.33
LB 2	65100	1500	7.65	0.11	−15.12	0.18
GD 561	63000	2500	6.67	0.16	−13.59	0.27
PG 0834+501	56500	1500	6.98	0.12	−14.23	0.19
Feige 55	58000	1500	7.17	0.12	−14.23	0.21
Feige 55	55000	1200	6.97	0.10	−13.93	0.19
PG 0134+181	56300	1300	7.40	0.11	−14.59	0.20
RE 1016−053	57500	1000	7.73	0.07	−15.01	0.15
PG 1413+015	49300	1100	7.70	0.10	−15.10	0.20
RE 2013+400	48900	1600	7.71	0.15	−15.13	0.29

observed profiles, it is necessary to discuss some uncertainties inherent to our calculations.

Bergeron et al. (1993) suggested that the Balmer-line problem could be resolved by including metal-line blanketing. Their calculations also indicated that the He II λ4686 line profile was not affected significantly in going from a metal-free fit to one including metallic ions (see their Figs. 1 and 4). Although Werner & Drezler (1993) reached different conclusions about the effect produced on the Balmer lines, they also show that the He II λ4686 line profile is not strongly affected by the inclusion of non-LTE metal-line blanketing in their calculations, with a line profile predicted somewhat deeper, but with an overall shape similar to the profile obtained from metal-free models. As discussed by Werner & Dreizler, the small difference observed in the line profiles can be compensated to some extent by decreasing the helium abundance in the metal-free model. In their 90,000 K, log g = 5.0 metal-free model, the helium abundance must be reduced from $N(\mathrm{He})/N(\mathrm{H}) = 0.1$ to 0.09 to match the line profile obtained from their full-fledged calculations. We thus conclude that metal-line blanketing has negligible effects on the predicted He II λ4686 line profile.

Napiwotzki & Schönberner (1993b) have shown that LTE calculations of the He II λ4686 line profile are comparable to non-LTE calculations, both in metal-free models, provided that the instrumental resolution is low enough that the line-core emission reversal is not spectroscopically resolved (this is certainly the case with our data set). Therefore, we conclude that the model spectra used here are perfectly appropriate to the analysis of the He II λ4686 line profiles and that full-fledged non-LTE calculations, including the effects of metal-line blanketing, would not affect substantially the following conclusions.

In Figure 4, we compare our best fits to the He II λ4686 line profiles with homogeneous and stratified composition models. The atmospheric parameters for each solution are those given in Tables 1 and 2. A close examination of each fit reveals that, in all cases, the homogeneous models provide a better match to the observed line profiles, which are intrinsically narrow and deep. In contrast, the profiles predicted from the stratified models are broad and shallow. The difference is more pronounced in the spectra with the stronger lines and higher signal-to-noise ratios (e.g., HZ 34, LS V+46 21, PG 0834+501). A similar conclusion was reached by Napiwotzki & Schönberner (1993b, Fig. 3) in the particular case of LS V+46 21. The results of Figure 4 clearly demonstrate that *the chemical composition of most DAO atmospheres is not stratified.* Therefore, the presence of helium in these objects cannot be explained as a result of a H/He abundance profile in diffusive equilibrium, as first suggested by Vennes et al. (1988) and expanded upon by MacDonald & Vennes (1991). Furthermore, although it is very difficult to imagine a physical process that could produce a complete homogeneous composition throughout the atmospheric regions, we must conclude that *the helium abundance distribution in the atmosphere of most DAO stars is homogeneous, at least in the helium-line–forming region.*

There is little information to be gained from the existing *IUE* observations of our DAO sample. In Figure 5, for

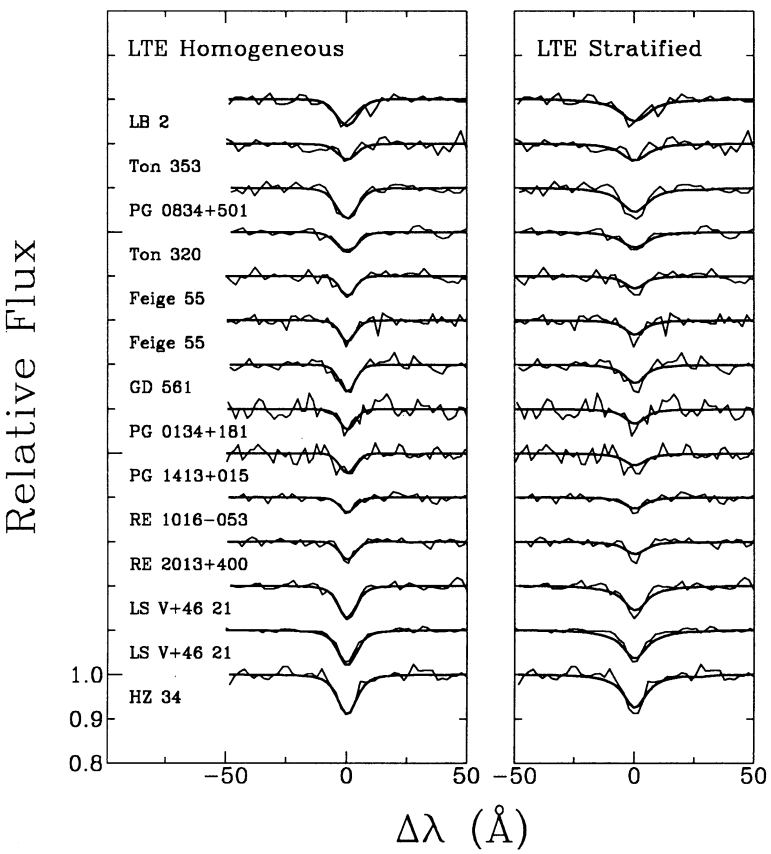

FIG. 4.—Our best fits to the He II λ4686 line using homogeneous and stratified composition models. The atmospheric parameters of each solution are given in Tables 1 and 2. These fits indicate that the line profiles are consistent with homogeneous models.

example, we display the archival *IUE* observations of these DAO stars and compare them with our homogeneous solutions (Table 1). The solid angle has been adjusted arbitrarily until a best fit is reached. Experiments with a normalization at V yield similar results. Comparisons with the stratified solutions of Table 2 are indistinguishable from those shown in Figure 5. Obviously, the He II λ1640 line profile cannot be used to infer the helium abundance distribution since the signal-to-noise ratio is clearly insufficient in most cases. These results indicate that our solutions, both homogeneous or stratified, are at least *consistent* with the *IUE* observations, with the single exception of PG 0134+181, for which the observed energy distribution is somewhat flatter than that predicted from our best optical solution.

Thus, our understanding of the helium abundance distribution in DAO stars rests on the analysis of a single He II line visible in their optical spectra. Our analysis is rather straightforward, however, and the uncertainties of our calculations are well understood. These small uncertainties will not change our main conclusion that the atmospheres of most, if not all, DAO stars are not stratified. Although stratified models seem more realistic from physical considerations, our analysis demonstrates that homogeneous models give a better description of the atmospheres of DAO stars.

4.4. *PG 1210+533 and PG 1305−017*

In the course of this analysis, PG 1210+533 and PG 1305−017 stood out as being special objects. Most notably, they are the two coolest DAO stars in our sample, with spectra exhibiting neutral helium lines as well as the characteristic He II λ4686 line. We therefore took advantage of the presence of these additional lines and modified our analysis in the following way. Instead of normalizing each line profile individually, we normalized the entire spectrum to a continuum set to

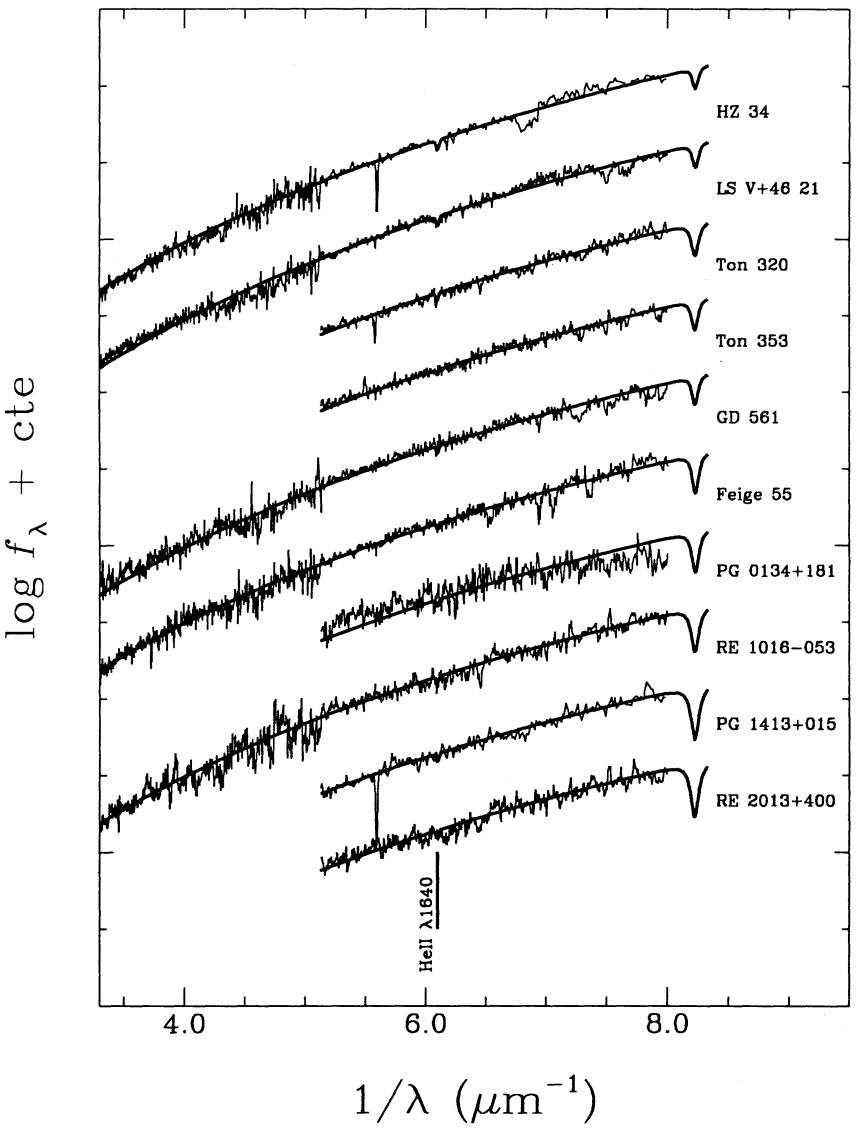

FIG. 5.—*IUE* energy distributions of DAO stars compared with theoretical spectra calculated from the homogeneous model parameters given in Table 1. Here, only the solid angle is adjusted until a best fit is reached; fits of comparable quality are reached if the energy distribution is normalized at V (when available) instead. Fits with stratified models are almost indistinguishable from those presented here. The fits are consistent with the ultraviolet observations, but these data provide no additional constraints.

TABLE 3

ATMOSPHERIC PARAMETERS OF PG 1210+533 AND PG 1305−017

A. HOMOGENEOUS MODELS

Name	$T_{\rm eff}$	$\sigma(T_{\rm eff})$	log g	σ(log g)	log y	σ(log y)
PG 1210+533	44800	400	7.89	0.04	−2.08	0.05
PG 1305−017	45700	600	7.70	0.12	−0.72	0.07

B. STRATIFIED MODELS

Name	$T_{\rm eff}$	$\sigma(T_{\rm eff})$	log g	σ(log g)	log $q_{\rm H}$	σ(log $q_{\rm H}$)
PG 1210+533	46600	400	7.91	0.04	−15.68	0.06
PG 1305−017	44400	400	7.76	0.10	−15.98	0.16

unity, and used all the information available. Again, we performed the analysis using both the homogeneous and stratified composition models.

The results for PG 1210+533 are presented in Figure 6 and Table 3. This comparison between the homogeneous and stratified fits is most puzzling. With both sets of models, the core of the He II λ4686 line is always predicted too shallow. This discrepancy is not related to our different fitting procedure since a similar result is reached even if the line profiles are fitted as above for the other DAO stars (see Bergeron et al. 1993, Fig. 1). The line wings, however, are better reproduced with homogeneous models, while they are predicted too broad with the stratified models (see the insert in Fig. 6). In contrast, our fit to the He I λ4471 line profile is somewhat superior with the stratified models. The Balmer lines are well reproduced otherwise, except perhaps for the very line core of Hβ. Our fits to the *IUE* observations displayed in Figure 7 are also inconclusive. In § 6, we discuss additional information as to the nature of this object.

The results for PG 1305−017 are presented in Figures 7 and

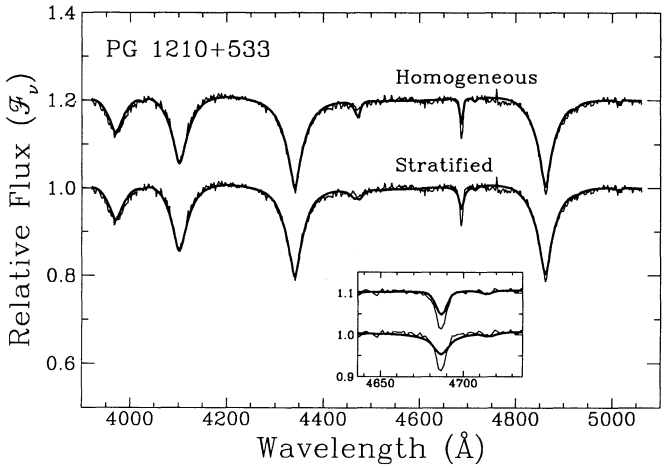

FIG. 6.—Our best fits to the optical spectrum of PG 1210+533 using homogeneous and stratified composition models. The atmospheric parameters of each solution are given in Table 3. Both the observed and theoretical spectra are normalized to a continuum set to unity. The top spectra are shifted by a factor of 0.2. The insert shows an enlargement of the region around He II λ4686. Neither the homogeneous nor the stratified solution provide a good match to the observed spectrum.

8, and reported in Table 3. Surprisingly, the fit with stratified models is in excellent agreement with the observed spectrum of this cool DAO star, whereas with homogeneous models, both the He II λ4686 and the He I λ4471 line profiles are predicted too deep, and the complex of H and He I lines around 4000 Å is not reproduced as well. Therefore, PG 1305−017 is the *only DAO star in our sample that shows evidence for stratification.* Again, not much information is gained from the *IUE* observations presented in Figure 7, other than to show that our solutions are consistent with the observed ultraviolet energy distribution.

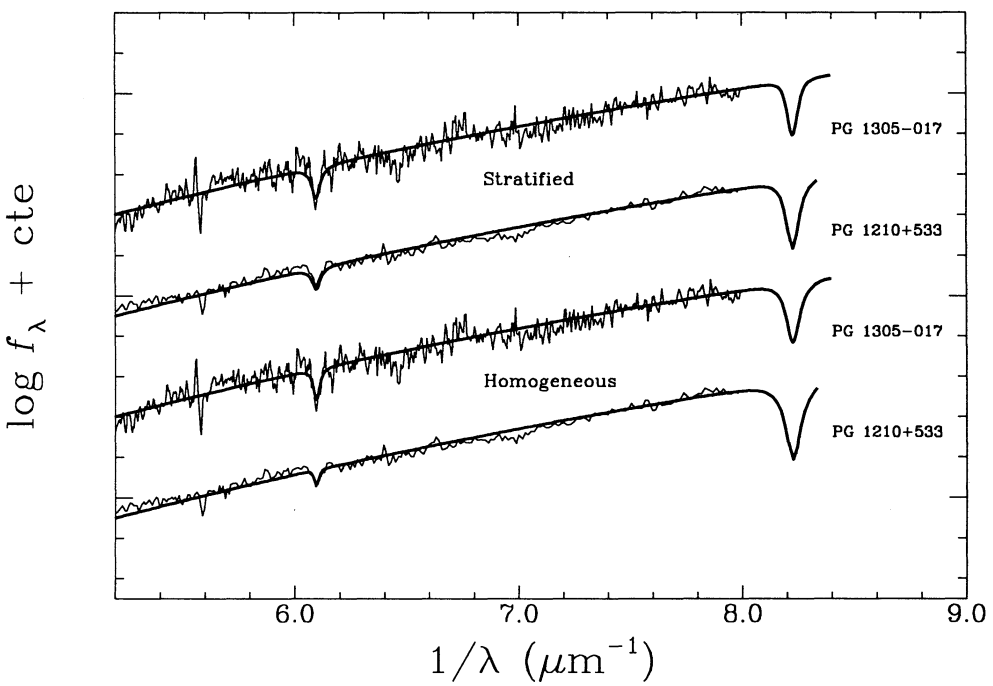

FIG. 7.—Our best fits to the *IUE* observations of PG 1210+533 and PG 1305−017 using homogeneous and stratified models. The atmospheric parameters are those obtained from the optical spectra (Table 3) and only the solid angle is adjusted until a best fit is reached.

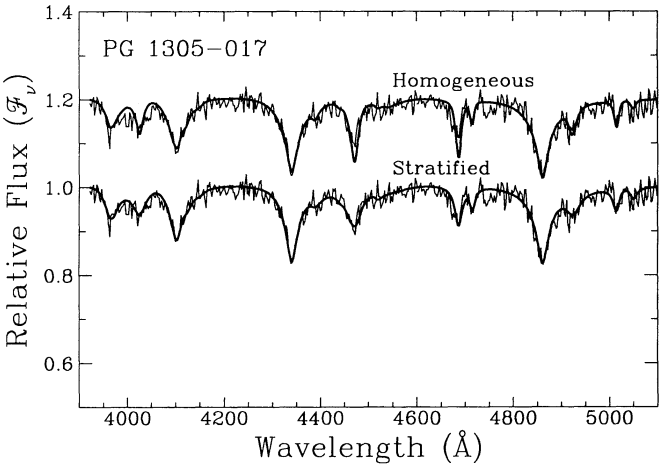

FIG. 8.—Same as Fig. 6, but for PG 1305−017. Here, a best fit is reached with the stratified solution.

It is worth noting parenthetically that our stratified fit for PG 1305−017 is in much better agreement with the observed optical spectrum than the stratified fits obtained by Koester, Liebert, & Saffer (1994) for the much cooler DAB star GD 323, and by Jordan et al. (1993) for the DAB star HS 0209+0832. Moreover, Wesemael et al. (1994) have shown that the two DAB stars discovered in the Montréal-Cambridge-Tololo survey were in fact composite DA + DB systems. PG 1305−017 thus represents the only convincing example of a hydrogen-dominated white dwarf with spectroscopic traces of helium that can be fit *successfully* with stratified composition models. What does differentiate this star from the hotter DAO stars, or for that matter from PG 1210+533, a DAO star with almost identical effective temperature and surface gravity? We defer our discussion to § 6, after we examine the atmospheric characteristics of DA stars in the same range of effective temperatures.

5. THE HOT DA STARS

5.1. *Sensitivity to the Assumed Atmospheric Composition*

Optical spectroscopic analyses of DA stars are usually performed with pure hydrogen models (see, e.g., BSL; Barstow et al. 1993a). However, since hydrogen is almost completely ionized in hot DA stars, even small traces of helium, even though spectroscopically invisible, can modify substantially the continuum opacity, and hence the optical continuum flux. Our results indicate that optical spectra calculated with homogeneous helium abundances as high as $N(\mathrm{He})/N(\mathrm{H}) \sim 10^{-5}$–$10^{-4}$ produce no detectable He II λ4686 feature (equivalent width smaller than $W_{4686} = 0.1$ Å) over the entire temperature range explored in this analysis. For comparison, most of our DAO stars have $W_{4686} \sim 0.5$ Å, while a $T_{\rm eff} = 60{,}000$ K, $\log g = 8.0$, and $N(\mathrm{He})/N(\mathrm{H}) = 10^{-3}$ model has $W_{4686} \sim 0.4$. We want to stress that such abundances of helium in the atmospheres of DA stars are not totally implausible. Vennes et al. (1988) have shown that helium is indeed radiatively supported in the photosphere of DA stars with equilibrium abundances of the order $N(\mathrm{He})/N(\mathrm{H}) \sim 10^{-5}$–$10^{-4}$ (see their Fig. 4). The only requirement, of course, is that helium be already present in the stellar envelope during the pre–white dwarf stage.

In the following, we assume a homogeneous abundance distribution of helium throughout the atmosphere. We ignore the fact that the true distribution is most likely given by the equilibrium profile between radiative acceleration and gravitational settling. In Table 4, we contrast the atmospheric parameters obtained with various helium compositions for the sample of DA stars selected by Wood & Bergeron (1994). The multiple observations of PG 1527+091 can be used to obtain an external error estimation, at least at the cool end of our sample. As suspected above, although this DA sample is restricted to white dwarfs classified DA1 in the McCook & Sion catalog, the objects are spread over a wide range of effective temperatures, reaching values as low as 20,000 K.

The most conspicuous result of our analysis is that the effective temperatures determined from fits to optical spectroscopy are extremely sensitive to the assumed helium composition. The $T_{\rm eff}$ determinations are most affected at the hot end of the sample, while the $\log g$ values remain relatively unaffected throughout. This result is illustrated in Figure 9, where we contrast the atmospheric parameters derived from pure hydrogen models to those obtained from helium-poor models. For statistical purposes, we are also making use in Figure 9 of the luminosity function sample, the results of which will be reported in due time.

According to Figure 9, a 52,000 K white dwarf with a (homogeneous) helium abundance of $N(\mathrm{He})/N(\mathrm{H}) = 10^{-4}$ could be interpreted as a 60,000 K white dwarf if it were analyzed under the assumption of a pure hydrogen composition. At higher temperatures, the effect is even stronger, reaching uncertainties as high as 25% around $T_{\rm eff} = 80{,}000$ K. Below $T_{\rm eff} \sim 40{,}000$ K, the observed sensitivity disappears. Interestingly enough, this is also the threshold temperature above which *ROSAT* studies of DA white dwarfs require additional opacities in the form of elements heavier than helium to account for the observations (Barstow et al. 1993a). It is thus entirely plausible that there is, in fact, *no* real "EUV flux deficiency" in many of the objects discussed by Barstow et al. We have experimented with *IUE* observations of some of these DA stars and found that it was impossible to discriminate between the pure hydrogen solutions and the helium-poor solutions given in Table 4.

Figure 9 indicates also that the surface gravities of DA stars are uniquely determined. While spectroscopic masses are usually derived from these $\log g$ estimates coupled with evolutionary models, the temperature uncertainties described above translate only into very small mass uncertainties. For example, a $\log g = 8.0$ white dwarf at $T_{\rm eff} = 80{,}000$ K is only $\sim 0.03\ M_\odot$ more massive than one at $T_{\rm eff} = 60{,}000$ K. We note also that there is no such uncertainty in the recent determination of the mass distribution of DA white dwarfs by BSL since nearly all stars in their sample have temperatures well below 40,000 K.

5.2. *Sample Fits*

In Figure 10, we show representative fits of the hottest objects in Table 4. We display only the solutions obtained from the pure hydrogen models; the fits obtained from the helium-poor models are indistinguishable from those. We also give masses for each star according to the evolutionary models of Wood (1990) for carbon core compositions ($q_{\rm He} = 10^{-4}$, $q_{\rm H} = 0$). The most surprising feature of these fits is that *none of the DA stars exhibits the Balmer-line problem reported in DAO stars.* The same conclusion applies to the other DA stars in Table 4, as well as to the ~126 additional DA stars from the luminosity function sample (not displayed here). The only problem encountered occasionally is a partial filling of the

TABLE 4

ATMOSPHERIC PARAMETERS OF HOT DA STARS

NAME	$y = 0$				$y = 10^{-5}$		$y = 10^{-4}$	
	$T_{\rm eff}$	$\sigma(T_{\rm eff})$	log g	σ(log g)	$T_{\rm eff}$	log g	$T_{\rm eff}$	log g
PG 1342+444	78700	2700	7.82	0.11	70600	7.83	59800	7.83
Ton 21	77300	1400	7.78	0.06	69800	7.79	59200	7.79
PG 1141+078	66000	1100	7.57	0.06	59400	7.57	54600	7.55
G191-B2B	64100	700	7.69	0.04	58200	7.69	53900	7.68
HZ 43	60700	1500	7.78	0.09	55800	7.78	52500	7.78
LB 335	60200	1000	8.33	0.06	56600	8.33	52500	8.32
PG 1234+482	57000	700	7.91	0.04	53500	7.92	50800	7.91
KUV 08026+4118	54000	800	7.53	0.06	50700	7.53	49400	7.53
GD 257	48100	470	7.83	0.04	46500	7.83	45500	7.83
PG 1642+386	47400	700	7.64	0.06	45800	7.64	45100	7.63
PG 0916+065	45400	500	7.73	0.05	44300	7.72	43600	7.72
PG 1057+719	42700	320	7.97	0.03	42000	7.97	41400	7.97
GD 153	40000	360	7.89	0.03	39500	7.88	39100	7.88
PG 1603+432	37600	230	7.97	0.03	37300	7.97	37000	7.97
PG 1636+351	37400	240	8.05	0.03	37100	8.05	36800	8.05
PG 1026+454	36500	190	7.87	0.03	36300	7.87	36100	7.86
PG 0937+506	36200	180	7.86	0.03	36000	7.85	35800	7.85
LB 2318	35900	300	7.85	0.05	35700	7.85	35600	7.85
GD 336	34800	190	8.05	0.04	34800	8.05	34600	8.05
Feige 93	34400	140	7.31	0.03	34300	7.31	34200	7.31
GD 80	33700	110	8.26	0.02	33700	8.26	33600	8.25
GD 71	33600	100	7.84	0.02	33500	7.84	33400	7.84
PG 1223+478	31300	160	7.80	0.04	31300	7.80	31300	7.80
PG 1620+648	30800	100	7.75	0.03	30800	7.75	30900	7.75
GD 200	28800	140	7.75	0.03	28800	7.75	28900	7.74
PG 0846+557	27900	150	7.82	0.03	27900	7.82	28000	7.82
PG 1120+439	27600	110	8.31	0.02	27700	8.31	27700	8.30
PG 1058−129	24900	110	8.70	0.02	24900	8.70	25000	8.70
PG 1527+091	21600	190	7.90	0.03	21600	7.90	21700	7.90
PG 1527+091	21400	220	7.92	0.03	21400	7.92	21500	7.92

lower Balmer-line cores by the emission from an unresolved cool companion. HZ 43 is such an object with a companion of spectral class dM3.5e (Margon et al. 1976). In this case, the atmospheric parameters may be significantly in error since the spectrum of the DA star is not deconvolved from the composite spectrum prior to fitting the line profiles. Indeed, Napiwotzki et al. (1993) attempted to deconvolve the two components of the HZ 43 system and obtained an effective temperature of $T_{\rm eff} = 49{,}000$ K, which is significantly cooler than ours. On the basis of *EXOSAT* data, Vennes & Fontaine (1992) found $T_{\rm eff} \sim 52{,}000$ K.

G191-B2B is probably the DA star analyzed most repeatedly in the literature, mainly because it is one of the brightest white dwarfs in the sky, and also because it is frequently used as a spectrophotometric standard. Surprisingly, the atmospheric parameters obtained for this object vary widely from one analysis to another. One of the latest estimates quoted in Barstow et al. (1993a) comes from the upcoming analysis of Finley, Koester, & Basri (1994). Their effective temperature ($T_{\rm eff} = 57{,}314 \pm 750$ K) and surface gravity (log $g = 7.497 \pm 0.065$) are significantly different from those derived here ($T_{\rm eff} = 64{,}100 \pm 700$ K, log $g = 7.69 \pm 0.04$). Our solution corresponds to a predicted trigonometric parallax of $\pi = 0''.0216 \pm 0''.0008$ (see BSL for details), in excellent agreement with the observed value of the trigonometric parallax given in van Altena, Lee, & Hoffleit (1993), $\pi = 0''.0225 \pm 0''.0022$. The earlier USNO measurement of Harrington & Dahn (1980), $\pi = 0''.0219 \pm 0''.0026$, agrees very sell with that value. The value derived from the solution of Finley et al. (1994), $\pi = 0''.0197 \pm 0''.0009$, is significantly smaller, but still consistent with the observed value. The predicted trigonometric parallax estimate depends strongly on the log g determination which favors a somewhat higher surface gravity for G191-B2B than estimated, e.g., by Finley et al. (1994; log $g = 7.497$) or Kidder (1991; log $g = 7.45$). We note also that our log g determination is in perfect agreement with the value of log $g = 7.69 \pm 0.22$ quoted in Finley et al. (1990), based on the gravitational redshift measurement of Reid & Wegner (1988).

5.3. *Implications for X-Ray and EUV Analyses*

Recent analyses of soft X-ray observations either from *Einstein*, *EXOSAT*, or *ROSAT* satellites, as well as upcoming analyses of extreme ultraviolet (EUV) data with *EUVE*, are confronted with the problem of constraining simultaneously a large number of free parameters such as $T_{\rm eff}$, log g, N(He)/N(H) (or $q_{\rm H}$), the hydrogen column density $N_{\rm H}$, and the value of the solid angle. To overcome this problem, these studies make extensive use of independent $T_{\rm eff}$ and log g determinations obtained from optical spectroscopic analyses, most of which are carried out using pure hydrogen models. Inference about the chemical composition and/or stratification is then drawn with the temperature fixed at the optical value. As discussed above, these optically determined temperatures are strongly dependent on the particular assumptions about the chemical composition. We show below that, for a consistent analysis, the optical and X-ray (or EUV) observations need to be considered *simultaneously*.

As an example, we consider a white dwarf with $T_{\rm eff} = 52{,}000$ K, log $g = 8.0$, and a homogeneous helium abundance of

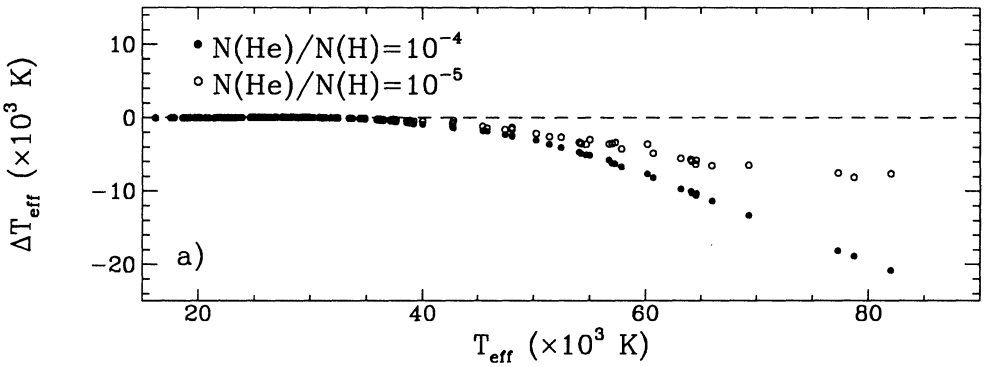

FIG. 9a

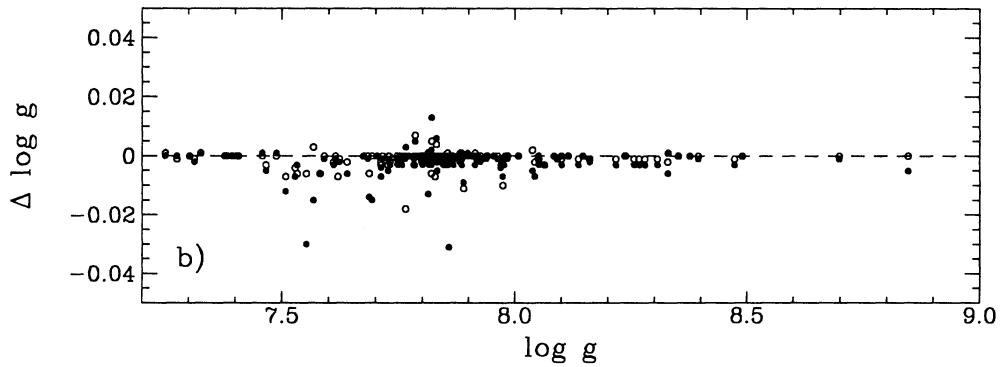

FIG. 9b

FIG. 9.—(*a*) Differences between the temperatures obtained from homogeneous helium-poor and helium-free models, as a function of the temperatures derived from pure hydrogen models. The various homogeneous helium compositions considered are indicated by different symbols. (*b*) Same as (*a*) but for surface gravity determinations. Effective temperatures are strongly affected by the presence of helium, whereas log g determinations are relatively unaffected.

N(He)/N(H) = 10^{-4}. According to Figure 9, a line profile analysis of this star with pure hydrogen models would yield a higher temperature of $T_{\rm eff} \sim 60{,}000$ K, but the same value of log $g = 8.0$. The standard procedure is then to normalize both the observed and model spectra at V and vary the helium abundance, with the temperature fixed at the optically determined value derived from pure hydrogen models, until a best fit to the EUV and soft X-ray observations is achieved. A simulation of this procedure is illustrated in Figure 11 for the range of wavelengths covered by *EUVE* and *ROSAT*. It is clear that a simultaneous fit, shortward and longward of the He II λ228 absorption edge, cannot be achieved for any assumed helium abundance. The flux absorbed shortward of 228 Å is redistributed longward of the edge where the opacity is smaller. Furthermore, if we consider only the regions shortward of 228 Å, where all the *ROSAT* observations have been obtained (no P2 data covering the 500–730 Å range were available for the stars studied by Barstow et al. 1993a), it is still not possible to reach an acceptable fit to the energy distribution. The best solution at log N(He)/N(H) ~ -3.5 is clearly not an acceptable one. Such an inconsistency would have been considered as conclusive evidence that this star cannot be fit with homogeneous models.

We now briefly summarize our results with stratified models. Although optically determined temperatures are also sensitive, for identical reasons, to the assumed value of $q_{\rm H}$ (see, e.g., the analysis of G191-B2B by Barstow et al. 1993b), the implications of EUV and soft X-ray analyses are less dramatic. The $q_{\rm H}$ value of a DA white dwarf cannot be arbitrarily small if it is to be detected by *ROSAT*. We adopt as a lower limit a value of log $q_{\rm H} \sim -14.5$ (for log $g = 8.0$), according to the results of Barstow et al. (1993a). This value is sufficiently "thick" that the regions where most of the optical radiation emerges have an almost pure hydrogen composition. Consequently, the effect on the temperature determination is less severe. For example, such a stratified white dwarf with $T_{\rm eff} = 56{,}000$ K would be interpreted as a $T_{\rm eff} = 60{,}000$ K white dwarf from a line profile analysis with pure hydrogen models. A simulation similar to that performed with homogeneous models is displayed in Figure 12. Again, it is not possible to achieve a simultaneous fit to the EUV and X-ray observations, although a good fit can be obtained if the analysis is restricted to the soft X-ray wavelength range.

These experiments stress the important issue first raised by Vennes, Shipman, & Petre (1990) that *the reality of the EUV/soft X-ray flux deficiency in hot DA stars is critically dependent on the accuracy with which the effective temperature is determined.* Finally, we note that the initial results from *EUVE* reported by Finley et al. (1993) concern three white dwarf stars with effective temperatures much lower than the temperature where the effects of the helium abundance on the optically determined $T_{\rm eff}$ values become important ($T_{\rm eff} \sim 40{,}000$ K).

6. ON THE NATURE OF DAO STARS

6.1. *Assessment of the Atmospheric Parameter Uncertainties*

The results of our analysis of a large sample of DAO and hot DA stars allow us to draw some interesting conclusions about

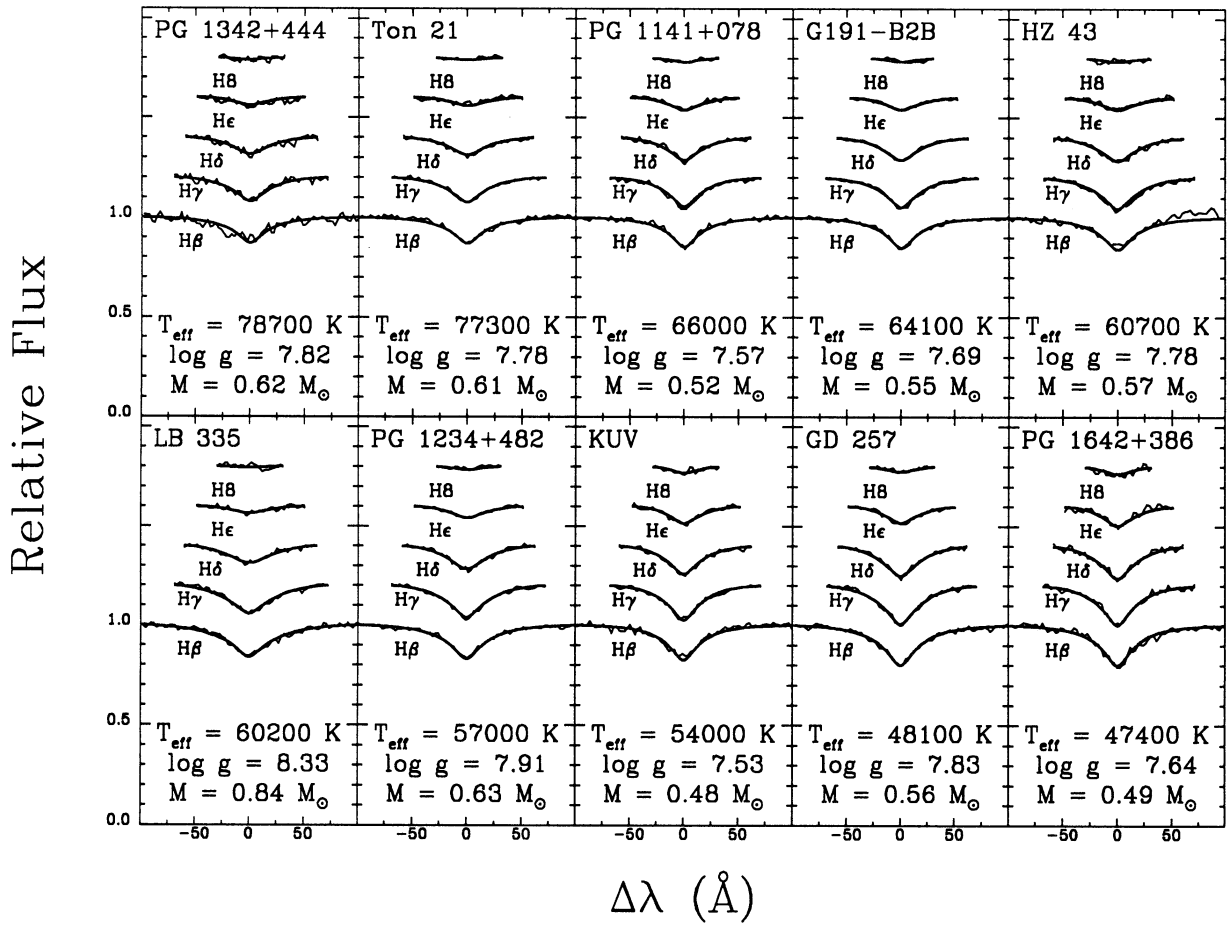

FIG. 10.—Fits to the individual Balmer lines for a representative subsample of hot DA stars using pure hydrogen models. In each panel, the lines are normalized to a continuum set to unity and offset vertically by a factor of 0.2.

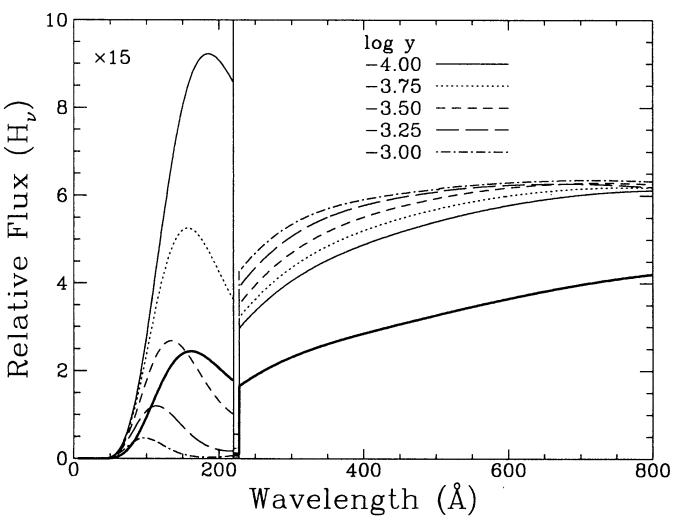

FIG. 11.—Energy distribution of a reference model with $T_{\rm eff}$ = 52,000 K, log g = 8.0, and N(He)/N(H) = 10^{-4} (*thick solid line*) compared with those of models with $T_{\rm eff}$ = 60,000 K, log g = 8.0, and with helium abundances as indicated on the figure. All the energy distributions are normalized to unity at V. The fluxes shortward of 220 Å are multiplied by a factor of 15 for clarity. The optical line profiles of the reference models are identical to those of a pure hydrogen model at $T_{\rm eff}$ = 60,000 K and log g = 8.0. For clarity, the line opacity has been neglected in the calculation of these energy distributions.

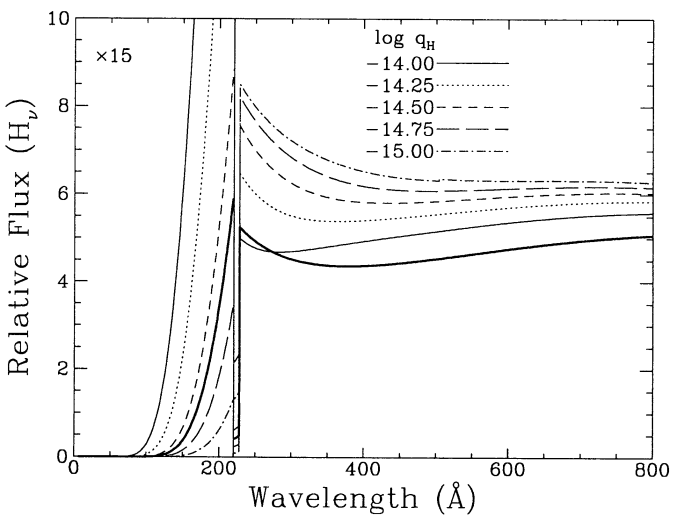

FIG. 12.—Energy distribution of a reference model with $T_{\rm eff}$ = 56,000 K, log g = 8.0, and log g = −14.5 (*thick solid line*) compared with those of models with $T_{\rm eff}$ = 60,000 K, log g = 8.0, and values of log $q_{\rm H}$ as indicated on the figure. All the energy distributions are normalized to unity at V. The fluxes shortward of 200 Å are multiplied by a factor of 15 for clarity. The optical line profiles of the reference model are identical to those of a pure hydrogen model (or alternatively, with an infinitely thick hydrogen layer) at $T_{\rm eff}$ = 60,000 K and log g = 8.0. For clarity, the line opacity has been neglected in the calculation of these energy distributions.

the nature and evolution of DAO stars. In Figure 13, we show the location of the DAO and the hottest DA stars in the ($T_{\rm eff}$, log g)-plane, including some from the luminosity function sample. For the DA stars, we display the results obtained from pure hydrogen models and also from models with a helium abundance of $N({\rm He})/N({\rm H}) = 10^{-4}$. For stars with multiple observations, a simple average of all parameters is used. The cooling sequences of Wood (1990, 1994) for carbon core compositions with $q_{\rm He} = 10^{-4}$ and $q_{\rm H} = 0$ are indicated as well. To show the effect of adding a thick hydrogen layer, a 0.55 $M_\odot$ sequence with $q_{\rm He} = 10^{-2}$ and $q_{\rm H} = 10^{-4}$ is also displayed. We now discuss some uncertainties inherent to the location of DA and DAO stars in this diagram.

While the surface gravities of the DA stars are uniquely determined (see Fig. 9), the derived effective temperatures can be lowered if traces of helium are present in their atmospheres. For instance, the hottest DA stars in Figure 13 have optically determined temperatures around 80,000 or 60,000 K when they are analyzed with pure hydrogen models or with homogeneous models with $N({\rm He})/N({\rm H}) = 10^{-4}$, respectively. Although the presence of helium in undetermined quantities probably dominates the uncertainty of the temperature determinations, the presence of heavier elements in the atmospheres of DA stars may also contribute to increase this uncertainty, as discussed below.

For the DAO stars, the uncertainties of each fitted parameter are more difficult to assess since a complete understanding of the Balmer-line problem has not yet been reached. If we attribute this problem to the presence of heavy elements, as suggested by Bergeron et al. (1993), we can estimate, at least for Feige 55, the magnitude of the uncertainty in each parameter by comparing their results from metal-line–blanketed models with those obtained here from metal-free models. Their analysis, based upon an approximate treatment of LTE metal-line blanketing, yields $T_{\rm eff} = 60{,}340$ K, log $g = 7.25$, and log $N({\rm He})/N({\rm H}) = -3.3$, assuming a homogeneous abundance composition. These determinations can be compared with those given in Table 1: $T_{\rm eff} = 58{,}300$ K, log $g = 7.15$, and log $N({\rm He})/N({\rm H}) = -2.92$ (the spectrum used by Bergeron et al. is that corresponding to the first set of values in Table 1). The helium abundances are comparable considering that Bergeron et al. (1993) used a cruder treatment of the He II λ4686 line profile calculation, while we are making use here of the detailed calculations of Schöning & Butler (1989). The surface gravity determinations are in fair agreement as well. Our effective temperature determination, however, is about $\sim$2000 K cooler, a difference which probably reflects the small back-warming effect of the deeper layers caused by metal-line blanketing (Bergeron et al. 1993; Dreizler & Werner 1993; Werner & Dreizler 1993). We note also that this difference in temperature determinations has been reduced significantly by considering only the line wings in our fitting procedure: In Bergeron et al. (1993), the difference in $T_{\rm eff}$ between their fit with metal-free models, including the entire line profiles, and those with metal-line–blanketed models is $\sim$6000 K, or about 3 times larger. Although we are unable to estimate the temperature uncertainties for all DAO stars individually, we can still conclude that the temperatures derived from our metal-free models are lower limits to the actual temperature of the star and that our log g and $N({\rm He})/N({\rm H})$ determinations remain fairly accurate.

6.2. *The Origin of DAO Stars*

We first consider the DAO stars shown as filled circles in Figure 13 (the others are considered separately in §§ 6.3 and 6.4). These nine objects are characterized by fairly high effective temperatures ($T_{\rm eff} \gtrsim 55{,}000$ K) and unusually low surface gravities. Allowing for uncertainties in the derived parameters, an imaginary boundary can be drawn in the ($T_{\rm eff}$, log g)-plane which separates these DAO stars from the higher gravity DA

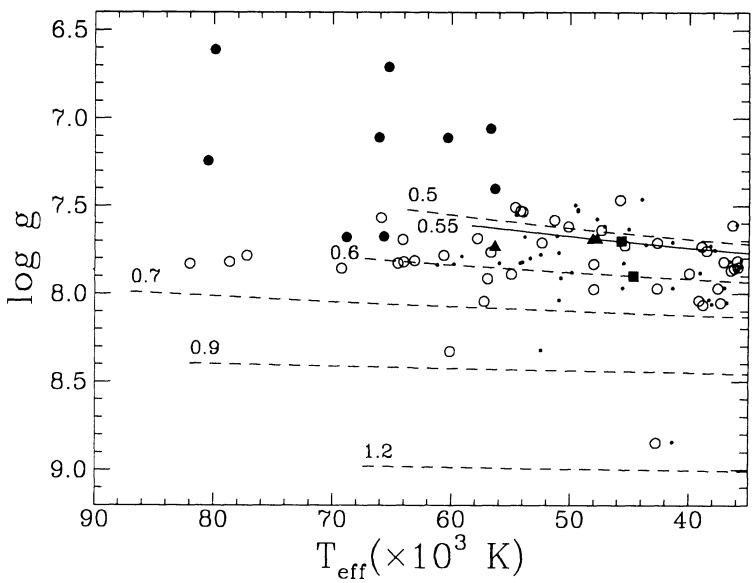

FIG. 13.—($T_{\rm eff}$, log g)-diagram for all the DAO and the hottest DA stars analyzed in this paper, as well as those from the luminosity function sample. The open circles correspond to the DA values obtained from pure hydrogen models, while the small dots assume a helium abundance of $N({\rm He})/N({\rm H}) = 10^{-4}$. The filled symbols correspond to the DAO stars: in particular, RE 2013+400, RE 1016−053, and PG 1413+015 are indicated by filled triangles, and PG 1210+533 and PG 1305−017 by filled squares. Also displayed are cooling sequences of Wood (1990, 1994) for carbon core compositions with $q_{\rm H} = 0$ (*dashed curves*), and a 0.55 $M_\odot$ sequence with a thick hydrogen layer of $q_{\rm H} = 10^{-4}$ (*solid curve*). Each sequence is labeled by its corresponding value of the mass.

stars. If one further assumes that a moderate helium abundance is present in the atmospheres of DA stars, this division becomes even more pronounced. We thus conclude that *hot, low surface gravity, single DA white dwarfs are necessarily DAO stars*. The opposite statement that all DAO stars are hot and have low surface gravities is not true, however, since there exist several cool DAO stars with normal surface gravities (see Fig. 13).

Two of the hot, low-gravity DAO stars, LS V+46 21 and GD 561, have been identified as central stars of planetary nebulae (CSPN), as discussed in § 2. The location of LS V+46 21 in Figure 13 (the hottest DAO at log $g \sim 7.2$) is entirely consistent with evolutionary models of post–asymptotic giant branch (AGB) stars. For example, we show in Figure 14 the evolutionary sequences of 0.546, and 0.605 $M_\odot$ post-AGB stars taken from Figure 5 of Napiwotzki & Schönberner (1991, Fig. 5).[5] The locations of Ton 320 and LB 2 would be consistent with this interpretation as well, although no planetary nebulae has yet been detected around these objects. Their planetary remnants could be so old and diffuse, however, that they may no longer be detectable.

The location of GD 561 in these diagrams ($T_{\rm eff} = 65{,}300$ K, log $g = 6.71$), however, is at odds with such an interpretation. Indeed, there is no post-AGB evolutionary model that evolves through this region of the ($T_{\rm eff}$, log g)-plane. Napiwotzki & Schönberner (1993a) identified GD 561 as the central star of the planetary nebula S174 from distance considerations, despite the fact that GD 561 is located far from the center of the nebula. Their derived atmospheric parameters are entirely consistent with ours. Since GD 561 is too hot and low in log g for its mass (or radius) to be evaluated directly from the evolutionary models of Wood (1994), we assume a value 0.5 $M_\odot$ (see next paragraph) and derive an absolute visual magnitude of $M_V = 5.97$. Therefore, our distance estimate for GD 561 is about 512 pc, a value which is not inconsistent with the somewhat uncertain nebular distance of S174, 220 $\pm$ 520 pc, derived from the Galactic rotation law (Fich & Blitz 1984). Since Napiwotzki & Schönberner presented evidence that S174 is indeed a planetary nebula instead of an H II region, as suggested by Fich & Blitz, we conclude that if GD 561 is the central star of S174, its origin cannot be explained by post-AGB evolution. We note finally that our close inspection of the plates from the Palomar Observatory Sky Survey did not reveal the presence of any nebulosity around the other DAO stars in our sample, except of course around LS V+46 21.

There are six DAO stars (including GD 561) in our sample with surface gravities low enough that their origin cannot be attributed to post-AGB evolution. Indeed, the minimum mass for reaching the thermally pulsing stage on the AGB is about 0.53–0.55 $M_\odot$ (Schönberner 1983; Dorman, Rood, & O'Connell 1993). According to the results of Figures 13 and 14, all six objects have masses significantly below 0.50 $M_\odot$ if they have relatively thin[6] hydrogen layers, or below 0.55 $M_\odot$ if they have thick hydrogen layers. Consequently, a different evolutionary channel needs to be invoked to account for these

[5] The 0.546 $M_\odot$ post-AGB evolutionary sequence has a thick ($q_{\rm H} \sim 10^{-4}$ $M_\odot$) hydrogen layer, and therefore the match with white dwarf cooling models should be made with the $q_{\rm H} = 10^{-4}$, 0.55 $M_\odot$ sequence displayed in Fig. 14. The slight residual mismatch is a result of neglecting the Coulomb effects in the post-AGB models of Schönberner (1983; see Koester & Schönberner 1986 for details).

[6] Evolutionary models with thin hydrogen envelopes ($q_{\rm H} \lesssim 10^{-8}$) are comparable to those with $q_{\rm H} = 0$ used in Figs. 13 and 14.

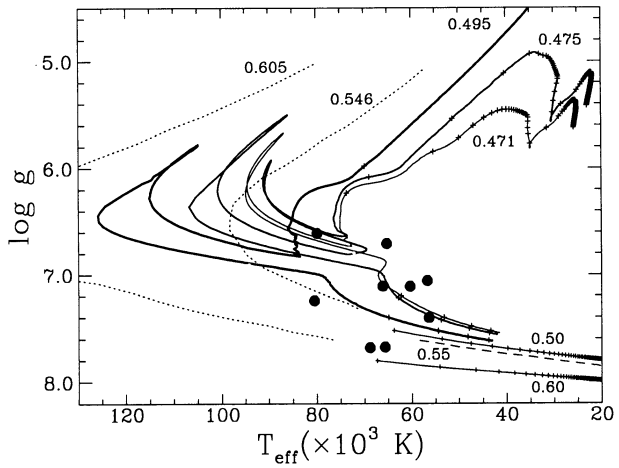

FIG. 14.—Location of the DAO stars (shown as filled circles in Fig. 13) in the ($T_{\rm eff}$, log g)-diagram, compared to that of the 0.5 and 0.6 $M_\odot$ ($q_{\rm H} = 0$; *solid curves at bottom right*) and 0.55 $M_\odot$ ($q_{\rm H} = 10^{-4}$; *dashed curves at bottom right*) white dwarf cooling sequences of Wood (1990, 1994), the post-EHB sequences of Dorman et al. (1993; *solid curves starting at upper right*), and the 0.546 and 0.605 $M_\odot$ post-AGB evolutionary sequences displayed in Napiwotzki & Schönberner (1991, Fig. 5; *dotted curves*). All sequences are labeled by their corresponding value of the mass, while the (+) signs mark time intervals of 10^6 yr, when available. Note that the temperatures of these DAO stars represent only lower limits (see text).

objects. We argue that hot subdwarf stars are the most likely progenitors of these DAO stars. Even though it is widely accepted that hot subdwarfs eventually evolve into white dwarf stars, the details of this evolution are still being studied. The most recent analysis comes from Dorman et al. (1993) who calculated an extensive grid of models for stars evolving from the extended (or extreme) horizontal branch (EHB), i.e., stars on the horizontal branch that do not reach the thermally pulsing stage on the AGB. Among those, the so-called AGB-manqué stars are of significant interest. These objects have hydrogen envelope masses that are small enough that, after core helium exhaustion on the EHB, they never evolved toward the AGB. Instead, they always remain at high effective temperatures ($T_{\rm eff} \gtrsim 20{,}000$ K) throughout their evolution.

Two post-EHB evolutionary sequences at 0.471 and 0.475 $M_\odot$ are displayed in Figure 14, together with a 0.495 $M_\odot$ sequence of the so-called post–early asymptotic giant branch (post-EAGB) stars. The latter objects leave the AGB before reaching the thermally pulsing stage (see Dorman et al. 1993 for details). All sequences were taken from the [Fe/H] = 0 models of Dorman et al. (1993). Since the temperature determinations of the low-gravity DAO white dwarfs are lower limits (see above), the location of these stars in Figure 14 is entirely consistent with post-EHB evolution. The only exceptions are the three hot DAO stars which we previously interpreted as post-AGB stars. Even the 0.495 $M_\odot$ post-EAGB sequence yields temperatures and surface gravities that are too high to account for most of the low-mass DAO stars. Therefore we conclude that the immediate progenitors of these DAO stars are post-EHB stars. Since the hot hydrogen-rich B and OB subdwarfs are associated with the bluest stars on the EHB, we also conclude that hot subdwarfs represent the even-earlier progenitors of these low-mass DAO stars. If our interpretation is correct, their corresponding masses are $M \sim 0.48$ $M_\odot$ (i.e., consistent with objects with very little mass beyond that required to ignite the degenerate helium core). We refrain from

speculating about the hydrogen-deficient subdwarf (sdO) stars since these objects are found in a wide range of (uncertain) $T_{\rm eff}$ and log g values, and they obviously do not form a homogeneous class of objects. Consequently, their evolutionary status cannot be easily interpreted, at this stage, within the present context.

The loops at high temperatures of each low-mass sequence in Figure 14 are associated with hydrogen-shell flashes (H-flashes) in rather thin envelopes. According to the results of Dorman et al. (1993), these occur only for a metallicity at or below solar. It is not clear if these H-flashes are real, however, since the timescales for these excursions are extremely short, and detailed computations require time steps of ~ 10 yr or so (B. Dorman, private communication). Dorman et al. (1993) further mention that these H-flashes have been observed in other independent evolutionary calculations as well (see references therein). It is worth noting that the location of GD 561 is entirely consistent with post-EHB evolution and that it lies very close to the region where these stars are believed to undergo H-flashes. It is thus tempting to associate the existence of a planetary nebula around GD 561 with such a phenomenon. This could be a strong indication that mass ejection in the form of a planetary nebula is not invariably associated with post-AGB evolution alone.

It is of some interest to verify whether the number of DAO stars in our sample, which were interpreted here as the result of post-EHB evolution, is consistent with birthrates determined for various pre–white dwarf channels. This can be accomplished by first calculating space densities for each sample. For that purpose, we employ the method used by Wesemael et al. (1985). The first step is to define appropriate samples that are statistically complete. We thus consider here only those objects included in the Palomar-Green (PG) survey. The luminosity function sample contains all DA stars in the PG survey, including DAO stars as well. There is a handful of DA stars in the temperature range of interest for which no spectra were available. For these objects, we have relied on temperature and surface gravity determinations taken from the literature. Also, we restrict our space density estimate in the range of temperature where these low-mass DAO stars are observed. We adopt as a conservative estimate a range of $70{,}000 \gtrsim T_{\rm eff} \gtrsim 50{,}000$ K. The DAO stars which have been interpreted as post-AGB stars are included in the DA sample; we refer simply to this samples as the post-AGB sample. We have retained four DAO stars for the analysis (Ton 353, PG 0834+501, PG 0134+181, and Feige 55), and 19 DA stars. The DAO star PG 0950+139, which we have excluded from our analysis (see § 2), has an estimated temperature of $T_{\rm eff} = 70{,}000 \pm 7000$ K (Liebert et al. 1989). In addition, if we assume that PG 0950+139 suffers from the Balmer-line problem discussed above, its temperature may be even higher, and above the upper temperature boundary considered here for our statistical analysis.

For each object, we have calculated the absolute visual magnitudes M_V following the prescription of Wesemael et al. (1980), which were converted into M_B using approximate values of the color index $(B-V)$ based on our $T_{\rm eff}$ and log g estimates. These M_B values can then be used for comparison with the photographic B magnitudes of the PG survey. The objects are assumed to be distributed in a disk, with density that scales as $\exp(-z/z_0)$ in the direction perpendicular to the Galactic plane and a value of $z_0 = 250$ pc. Our computation yields space densities of 5.4×10^{-8} and 8.8×10^{-7} pc^{-3} for the low-mass DAO and post-AGB stars, respectively. We also need to include in the post-AGB sample, the contribution from the DO stars. Fortunately, the DO stars are found in a comparable range of effective temperatures, so that the results of Wesemael et al. (1985) can be used directly. For $z_0 = 250$ pc, Wesemael et al. (1985) found a value of 3.0×10^{-7} pc^{-3} for the DO stars. To derive birthrates, the last step is to estimate the evolutionary timescales for each group of stars. We make the assumption that the low-mass DAO stars all have a mass of 0.475 $M_\odot$ and use the evolutionary models of Dorman et al. (1993) to estimate the cooling timescale between $T_{\rm eff} = 70{,}000$ K and 50,000 K. For the other white dwarfs, we assume a mass of 0.6 $M_\odot$ and obtain an estimate of the evolutionary timescale from the models of Wood (1994). We find $\tau = 2.17 \times 10^6$ and 1.62×10^6 yr for the low-mass DAO stars and post-AGB stars, respectively. Combining these estimates, the corresponding birthrates are 2.5×10^{-14} and 5.4×10^{-13} pc^{-3} yr^{-1}. Therefore, about 4.6% of the white dwarf population is evolving from these low-mass DAO stars. This number is entirely consistent with earlier conclusions that only a very small fraction of the total population of white dwarfs has evolved from post-EHB stars (Drilling & Schönberner 1985; Heber 1986; Drilling 1992).

Finally, we note that a study of the kinematics of DAO stars, and a comparison with values derived from hot B and OB subdwarf stars (see Saffer 1991, and references therein), could potentially confirm our interpretation that DAO white dwarfs evolved from post-EHB stars. Precise radial velocity measurements for our sample of DAO stars are not yet available, however.

6.3. *The Presence of Helium in DAO Stars*

Since most DAO stars have fairly high effective temperatures and unusually low surface gravities, it would be tempting to interpret anew the presence of helium in DAO stars as the result of selective radiative pressure. The detailed calculations of Vennes et al. (1988), however, have convincingly demonstrated that this is not a viable explanation. Equilibrium abundances of helium expected at the photosphere of hot white dwarfs are always a factor of ~ 10 smaller than those determined here, even in a 0.4 $M_\odot$ white dwarf. Instead, stratified models were invoked there to explain the presence of helium in DAO stars (and hot DA stars as well). Unfortunately, stratified atmosphere models do not reproduce the details of the observed He II λ4686 line profile, as demonstrated in § 4.3. Therefore, another physical mechanism needs to be invoked to compete with gravitational settling and to support the observed helium abundances in DAO stars. Radiative acceleration and stratified configurations being ruled out, we argue that a weak mass loss may be a promising avenue of investigation.

Although there is no direct evidence for a stellar wind in most of our DAO stars, the existence of planetary nebula remnants around LS V+46 21 and probably GD 561 is a clear indication that mass loss is occurring at least in these objects. Furthermore, most CSPN in the list of Napiwotzki & Schönberner (1993a), identified as white dwarfs (such as Abell 7 and NGC 7293), are of the DAO spectral type. We thus speculate that the presence of helium in these DAO stars may be related to the presence of ongoing mass loss. Not all CSPN identified as white dwarfs in the list of Napiwotzki & Schönberner (1993a) are of the DAO spectral type, however. One glaring exception is WDHS1, for which Liebert et al. (1994) recently

obtained a high-quality spectrum which shows no detectable He II λ4686 feature. Their Balmer-line analysis indicates an extremely high effective temperature for this object ($T_{\rm eff} \gtrsim$ 100,000 K), but more importantly, the surface gravity of log $g \sim 7.6$ is significantly larger than the values derived for LS V+46 21 and GD 561. This could be an indication that the presence of helium in CSPN is correlated with their value of log g. This suggestion is reinforced by the recent analysis by Napiwotzki (1993), which reveals that all CSPN classified sdO/DAO have surface gravities of log $g \lesssim 7.0$, while those classified DA have log $g \sim 7.5$. This trend can be explained if mass loss is more efficient in producing helium enhancement in the atmospheres of low-gravity stars than in those of high-gravity stars. This is not unexpected if the wind is stronger in the more luminous objects. Alternatively, this trend can be explained if high-gravity CSPN have thicker hydrogen envelopes, and thus a helium reservoir buried deeper into the star.

Since mass-loss phenomena are far from being well understood in late stages of stellar evolution, one can easily argue that mass loss is also occurring for the other low-gravity DAO stars in Figure 14, a suggestion which offers a plausible explanation for the presence of helium in these stars as well. Furthermore, if these stars are indeed the result of post-EHB evolution, their total hydrogen content needs to be extremely small (Dorman et al. 1993), with the helium-rich envelope lying very close to the stellar surface. Note that mass loss has also been called upon to explain the presence of helium in the hydrogen-rich OB subdwarf stars; indeed detailed calculations of non-LTE radiative acceleration of helium in the atmospheres of sdOB stars by Michaud et al. (1989) reveal that the observed helium abundances in these stars cannot be supported by radiative acceleration alone, and that other processes, *such as mass loss*, must be involved.

The number of observed DAO stars decreases significantly at cooler temperatures, which suggests that helium eventually disappears from the photospheric regions as DAO white dwarfs cool off. This suggestion is strengthened by the fact that DA and DAO stars do not strongly overlap in the ($T_{\rm eff}$,log g)-plane. There are three exceptions, however (excluding PG 1210+533 and PG 1305−017 which are discussed below): RE 2013+400, RE 1016−053, and PG 1413+015 (shown as filled triangles in Fig. 13). These three objects have normal surface gravities (log $g \sim 7.7$), and their $T_{\rm eff}$ and log g values overlap comfortably with those of several DA stars. Their distinct location in the ($T_{\rm eff}$, log g)-plane, away from where the other DAO stars are normally found, suggests a different origin for these objects. Interestingly enough, all three stars are members of white dwarf + M dwarf composite systems! Tweedy et al. (1993) and Barstow et al. (1993c) suggested that binary star effects, such as accretion from the wind of the M dwarf component, could perhaps explain the presence of helium in the DAO component of such systems. Alternatively, one could argue that these systems are most likely the result of common-envelope evolution, and that mass transfer between the two components of the system has considerably reduced the total amount of hydrogen in the white dwarf remnant; any moderate mass loss would eventually bring some of the underlying helium-rich material to the surface. Further evidence is presented in § 7 that the DAO nature of these three stars, or, more explicitly, that the presence of helium in their atmosphere, can be attributed to the presence of, or to prior interaction with, the M dwarf companion.

Finally, we discuss some correlations observed among the atmospheric parameters of our DAO star sample (excluding again PG 1210+533 and PG 1305−017). Figure 15 displays all possible relations between the values given in Table 1. There is an apparent correlation between log g and log N(He)/N(H) (*bottom panel*), but since this result depends strongly on one determination, HZ 34 at log N(He)/N(H) = −1.33, we do not consider this correlation significant. The $T_{\rm eff}$ versus log N(He)/N(H) relation (*middle panel*), however, reveals that hotter stars tend to have larger helium abundances. This is a remarkable correlation considering that the presence of helium in these DAO stars has been explained with different origins. This relation can eventually be used to constrain models attempting to explain the presence of homogeneous abundances of helium in DAO stars. Since $T_{\rm eff}$ and log g (*top panel*) are also weakly correlated, it is not clear how the various atmospheric parameters interplay in governing the predicted

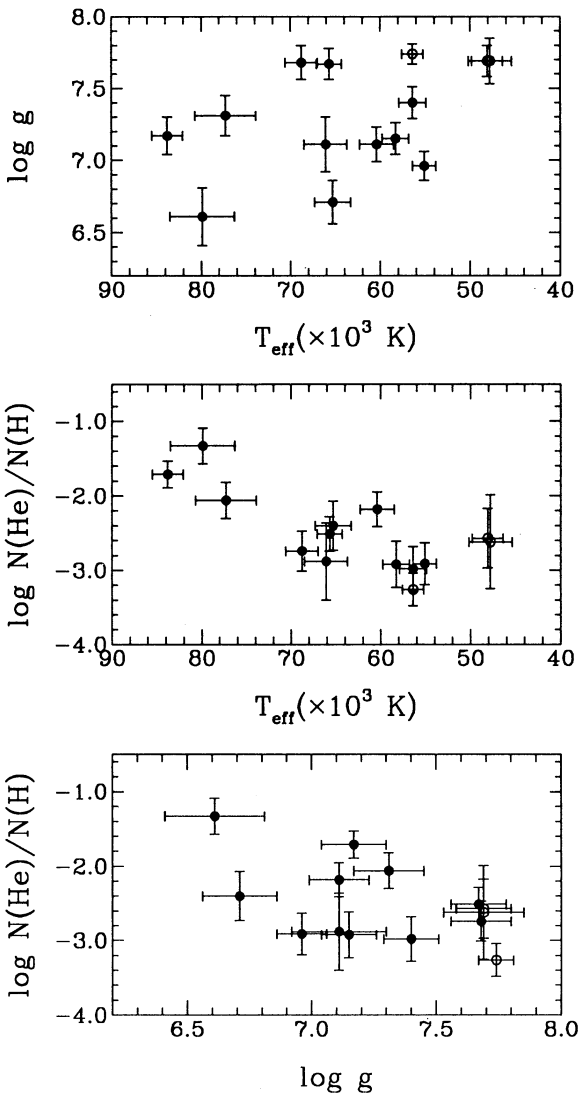

FIG. 15.—Correlations between the atmospheric parameters of DAO stars and corresponding uncertainties taken from Table 1 (excluding PG 1210+533 and PG 1305−017); multiple observations are considered individually. The DAO stars which are members of white dwarf + M dwarf composite systems are indicated by open circles.

helium abundance. Only detailed diffusion calculations along the lines of Chayer et al. (1993), which include mass loss and radiative acceleration, can answer these questions more quantitatively.

6.4. *The Nature of PG 1305−017 and PG 1210+533*

PG 1305−017 and PG 1210+533 are the coolest DAO stars in our sample, and the presence of helium in their atmosphere cannot be easily reconciled with any of the physical mechanisms considered above. We discuss these two objects in turn.

As discussed in § 1, DAO stars have in the past often been interpreted as intermediate objects between the hot helium-rich white dwarfs and the DA stars. Hydrogen thoroughly mixed in the envelope of the helium-rich progenitors would slowly diffuse toward the stellar surface and gradually enrich a helium atmosphere with hydrogen. If DAO stars represented such a transitory phase, not only should their atmosphere be stratified, a result ruled out by our analysis, but the inferred helium abundances should also be spread over a continuous range of values. An inspection of Table 1 reveals, on the contrary, that the helium abundances of DAO stars are confined to a very narrow range of values. We thus conclude that *most DAO stars are not transitional objects between the DO and the DA stars.*

PG 1305−017 represents a singular exception, however. The helium abundance inferred from homogeneous models, $\log N(\mathrm{He})/N(\mathrm{H}) = -0.72$, is significantly larger than that of the other DAO stars. This would be most unlikely, had PG 1305−017 evolved from a "normal" DAO star such as those studied here. The abundance of helium would have had to increase with time, whereas we expect DAO stars to become more hydrogen-rich and to eventually turn into DA stars. Instead, the spectrum of PG 1305−017 can be fit successfully with stratified models, a result consistent with the star being in diffusive equilibrium. We therefore suggest that *PG 1305−017 has evolved from a helium-rich DO white dwarf.* Its atmosphere is stratified as a direct consequence of the upward diffusion of hydrogen in the helium-rich atmosphere of its progenitor. The derived temperature also lies close to the blue edge of the so-called DB gap. If our interpretation is correct, the paucity of objects such as PG 1305−017 suggests that the timescale to transform a DO white dwarf into a DA star may be very short.

We are finally left with the puzzling case of PG 1210+533. This star has a temperature and a surface gravity very similar to those of PG 1305−017, although the helium abundance in PG 1210+533 is much lower, $N(\mathrm{He})/N(\mathrm{H}) \sim 10^{-2}$, a value more characteristic of the abundances found in hotter DAO stars. Since neither the stratified nor the homogeneous models can provide a satisfactory fit to the helium line profiles, the nature of PG 1210+533 remains ambiguous. Even more puzzling are the dramatic spectral changes observed in this object: In Figure 16, we compare our spectrum of PG 1210+533 (obtained in 1992) with those published by Wesemael et al. (1985), Holberg (1987), and Kidder (1991). Most noteworthy is the change in the strength of the He I λ4471 feature, and to a lesser extent of the He II λ4686 line. All spectra are consistent with the same values of $T_{\rm eff}$ and $\log g$, but with varying helium abundances of (from top to bottom in Fig. 16) $\log N(\mathrm{He})/N(\mathrm{H}) = -1.63$, -1.60, -1.52, and -2.08, respectively. In all fits, the observed He II λ4686 feature is always deeper than the model spectra, while the He I λ4471 line profile is better reproduced when the line is strong (as in the two middle spectra).

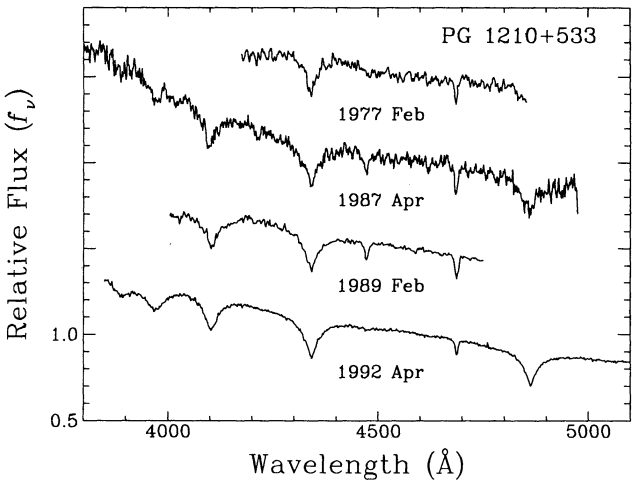

FIG. 16.—Comparison of our spectrum of PG 1210+533 (1992 April) with earlier spectra of the same star published by Wesemael et al. (1985; 1977 February), Holberg (1987; 1987 April), and Kidder (1991; 1989 February). Note the change in the strength of the He I λ4471 and He II λ4686 features.

Therefore, we conclude that the spectral changes observed in PG 1210+533 are not secular, but appear to be modulated in time. Further monitoring of PG 1210+533 is required before the nature of this object can be understood in greater detail.

The spectral variations of PG 1210+533 bear some resemblance to those observed in the magnetic white dwarf Feige 7 (Achilleos et al. 1992), in which they have been interpreted in terms of a rotating white dwarf with variable surface abundances of hydrogen and helium. Spectral variations are also thought to have occurred in the DAB star G104-27 in which the He I λ4471 and λ5015 features have clearly been identified by Holberg, Kidder, & Wesemael (1990), but have not been detected in following spectroscopic observations (Kidder et al. 1992). We note finally that there is no strong indication of any observed spectral variations in LS V+46 21 or Feige 55 displayed in Figure 1, or in any other DAO stars observed in common with Wessemael et al. (1985) and Holberg (1987). A possible exception is PG 0134+181, in which He II λ4686 had not been detected by Holberg (1987), although this result may be due to the lower signal-to-noise ratio of his observation.

7. THE BALMER-LINE PROBLEM IN DAO STARS

It is now possible from the results of our analysis to comment on the nature of the Balmer-line problem in DAO stars. We first note that this problem is encountered in all DAO stars contained in this low-gravity and high-temperature region of the ($T_{\rm eff}$, $\log g$)-plane (*filled circles* in Fig. 13). No obvious Balmer-line discrepancy is observed in any of the other cooler DAO stars. For RE 2013+400, the situation is ambiguous since the line cores are filled in emission by reprocessed material from the companion. Among the DAO stars which exhibit the Balmer-line problem, there is no strong correlation between the magnitude of the problem and the temperature and/or surface gravity of the star. Although Napiwotzki (1993) reported that the line discrepancy observed in Feige 55 was "weak" compared to that found in LS V+46 21, our results presented in Figure 3 indicate that the discrepancy is comparable in both stars, even though Feige 55 is ∼20,000 K cooler than LS V+46 21. Hence, the effective temperature of the star is *not* at the origin of the Balmer-line problem.

As demonstrated in our analysis, the Balmer-line problem is not present in any of the DA stars we have studied so far. One striking difference between the "problematic" DAO stars and the hot DA stars, aside from the obvious presence of helium in the former objects, is the log g range spanned by each group of stars. Although this may indicate that perhaps gravity is at the origin of the Balmer-line problem, a comparison between our fits to the low-gravity DA star PG 1141+078 and the DAO star Ton 320 reveals that the Balmer-line problem is seen only in the latter object, despite their comparable values of $T_{\rm eff}$ and log g (the surface gravity in PG 1141+078 is even lower than in Ton 320). Therefore, we also exclude surface gravity effects as the source of the Balmer-line discrepancy.

Since the Balmer-line problem is observed only in DAO stars, one could argue that the very presence of helium in these stars is at the origin of the discrepancy. We have shown, however, that simultaneous fits to all Balmer and helium lines could be achieved in the cooler, higher gravity DAO stars (*filled triangles* in Fig. 13). Hence, unless temperature and surface gravity effects compensate each other in some strange fashion, we believe that the presence of helium does not hold the key to the Balmer-line problem. Furthermore, our treatment of the helium opacity is straightforward, and the observed Balmer-line discrepancy is well beyond the theoretical uncertainties of our analysis. Even state-of-the-art, non-LTE models reported by Napiwotzki (1992) fail to reproduce the line profiles of LS V+46 21.

It is also very unlikely that the Balmer-line problem is connected to physical effects unaccounted for in the model calculation; otherwise, the discrepancy would be observed in DA stars as well, in the range of atmospheric parameters where DA and DAO stars slightly overlap. The effects of effective temperature, surface gravity, and helium abundance being ruled out, we are thus forced to conclude that there is a missing parameter in the analysis, and we reiterate our belief already expressed in Bergeron et al. (1993) that the presence of heavy elements is the most plausible explanation for the origin of the Balmer-line problem. If indeed, metal-line blanketing is the correct explanation, we expect a clear dichotomy between the abundances of heavy elements in DAO stars and those in DA stars, since the Balmer-line problem is not observed in any DA stars, while it is strong in almost all DAO stars. To that effect, we point out that the strength of the Balmer-line problem varies even between DAO stars with comparable $T_{\rm eff}$, log g, and N(He)/N(H) (e.g., Ton 320 and LB 2), a result which may imply slightly different metal abundances in each object.

If metal-line blanketing is at the origin of the problem, we have to conclude that the metallic abundances in RE 2013+400, RE 1016−053, and PG 1413+015, where the Balmer-line problem is *not* observed, are much smaller than in their hotter siblings. This conclusion is strengthened by the fact that RE 2013+400 and RE 1016−053 are the only DAO stars in our sample detected by *ROSAT* and *EUVE* (see below), even though they are both cooler than most of the DAO stars analyzed here, none of which were detected. PG 1413+015 is most likely too faint (V = 17.1) to have been detected. In the hotter, low-gravity DAO stars, we have invoked a small mass loss to account for the presence of helium. This mass loss coupled to selective acceleration of heavy elements could strongly affect the metallic content of their atmospheres, potentially leading to (over)abundance anomalies. Lamontagne et al. (1993) have shown indeed that the abundances of C, N, and Si in the DAO star Feige 55 are much larger than those derived in the hot DA white dwarfs Feige 24 and G191-B2B analyzed by Vennes, Thjell, & Shipman (1991). In contrast, since it has been suggested (see § 6.3) that the presence of helium in the three DAO stars discussed above could be the result of binary effects or past interaction with their companion, one could speculate that the metal abundances in these objects can be significantly different from the abundances encountered in the post-AGB and post-EHB DAO stars.

These important results also indicate that *heavy elements, instead of helium, provide most of the soft X-ray absorbing material in DAO stars.* This interpretation would explain the most peculiar result that none of the DAO stars in our sample were detected by *EUVE* in the first version of the Bright Source List (Malina et al. 1994), with the exception of RE 1016−053 (V = 14.3) and RE 2013+400 (V = 14.6). Indeed, a simple calculation indicates that in the $\lambda\lambda$230–800 region, the EUV flux of a typical metal-free DAO star at $T_{\rm eff}$ = 60,000 K, log g = 7.0, and a helium abundance as high as N(He)/N(H) = 10^{-2} is more than 6 times *larger* than that of a 40,000 K pure hydrogen white dwarf, many of which were detected by *EUVE* (we assume here that both stars have the same V magnitude). The same conclusions hold with stratified solutions. There are several bright DAO stars in our sample, GD 561 (V = 14.52), PG 0834+501 (V = 14.88), and most notably Feige 55 (V = 13.13) and LS V+46 21 (V = 12.67; Cheselka et al. 1993), none of which were detected by *EUVE*. It is clear that some additional opacity is required to account for the null detection of so many DAO stars by both *ROSAT* and *EUVE*. Metallic ions, in abundances significantly larger than those encountered in DA stars, are most likely the missing source of opacity and, consequently, the source of the Balmer-line problem in DAO stars.

As mentioned in § 4.1, the self-consistent, non-LTE, metal-line–blanketed model calculations of Werner & Dreizler (1993) show little effect on the predicted Balmer-line profiles. However, their analysis has been restricted, so far, to lower surface gravity models (log $g \lesssim 6.0$), with metal-line blanketing from C, N, O, and Fe only. In the face of what we believe to be overwhelming observational evidence, we believe that the parameter space needs to be explored even further, with the possible inclusion of additional metallic species, before the presence of these ions can be ruled out as the origin of the Balmer-line problem.

8. CONCLUSIONS

We have presented a thorough spectrophotometric analysis of DAO and hot DA stars. We have shown that the atmospheres of most DAO stars are not stratified, with only one exception, PG 1305−017. This surprising result suggests that some mechanism other than ordinary diffusion is competing with gravitational settling to support helium in the photospheric regions. In turn, this implies that thin hydrogen layers are not necessarily required to explain the existence of DAO stars. At least five subclasses of DAO stars have been identified, a result which suggests that this class, much like the DAB stars (Wesemael et al. 1994), might also be a rather inhomogeneous collection of objects: (1) those that are consistent with post-AGB evolution, (2) those which evolved from post-EHB stars, (3) those that are members of white dwarf + M dwarf composite systems, (4) at least one stratified white dwarf, PG 1305−017, which presumably evolved from a hot DO star, and (5) PG 1210+533, whose spectrum is variable as a possible result of surface abundance inhomogeneities.

For the first time, we believe we have identified white dwarfs whose origin can, rather convincingly, be traced back to hot subdwarfs: these are the low-mass ($M \lesssim 0.48\ M_{\odot}$) DAO stars whose mass is consistent with our current understanding of post-EHB evolution of hydrogen-rich subdwarf stars. Since we have found no evidence for hot, low-mass DA stars in our sample, we conclude that all low-mass post-EHB stars evolve into low-mass DAO stars. We have shown that the birthrate of this subsample of DAO stars is consistent with current estimated values of low-mass post-EHB birthrates. A significant fraction of the low-mass ($M \lesssim 0.5\ M_{\odot}$) stars in the mass distribution of BSL can certainly be assigned to the further cooling of these DAO stars. We have shown also that, in at least one object (GD 561), post-EHB evolution proceeds with episodes of mass loss in the form of planetary nebula–like ejection. This implies that planetary nebula cannot be directly associated only with post-AGB evolution until a detailed analysis of its central star is performed.

We have presented supporting evidence that the Balmer-line problem, which is only encountered in DAO stars, but not in all of them, is related to the presence of heavy elements in the atmosphere of these stars, with abundances that are significantly larger than those encountered in DA stars. We have suggested that these elements provide most of the soft X-ray and EUV opacity in DAO stars since the coolest (not necessarily the brightest) DAO stars have been detected by *ROSAT* and *EUVE*, while the hotter, more luminous ones were not. Simultaneously, the Balmer-line problem is observed only in this latter group of DAO stars, a result which lends strong support to our interpretation of the origin of this problem in these objects.

Since radiative acceleration alone cannot explain the observed helium abundance in DAO stars, we have invoked mass loss as a possible competitor to gravitational settling. This interpretation is not on firm ground, however, since detailed calculations are not yet available. Nonetheless, no matter what the competing mechanism might be, one has to consider the possibility that traces of helium, in somewhat smaller abundances, may be present in DA stars as well since radiative levitation *does* provide such minimal abundances (Vennes et al. 1988). Atmospheric parameters determined with models containing spectroscopically invisible traces of helium have been shown to differ significantly from those obtained with pure hydrogen models. This problem has been overlooked in the past, but may strongly affect the results and conclusions of soft X-ray and EUV analyses. In particular, we have demonstrated that optically determined temperatures need to be derived consistently with respect to the assumptions made about the atmospheric composition and/or structure.

We are grateful to M. S. Fulbright and R. A. Saffer for reducing some of the observing material used in this analysis, to B. Dorman for giving us easy access to his evolutionary models, to R. W. Tweedy, M. A. Barstow, and J. B. Holberg for giving us access to their spectrum of RE 2013+400, to J. B. Holberg for providing us with important unpublished material, and to P. Chayer for enlightening discussions. This work was supported in part by the NSERC Canada, by the Fund FCAR (Québec), and by NSF grants AST 92-17961 and AST 92-17988. M. A. W. also acknowledges financial support from the AAS Small Grant Program and the 1992–1993 Earnest F. Fullam Award of the Dudley Observatory.

REFERENCES

Achilleos, N., Wickramasinghe, D. T., Liebert, J., Saffer, R. A., & Grauer, A. D. 1992, ApJ, 396, 273
Barnard, A. J., & Cooper, J. 1970, J. Quant. Spectrosc. Rad. Transf., 10, 695
Barnard, A. J., Cooper, J., & Smith, E. W. 1974, J. Quant. Spectrosc. Rad. Transf., 14, 1025
———. 1975, J. Quant. Spectrosc. Rad. Transf., 15, 429
Barstow, M. A. 1989, in IAU Colloq. 114, White Dwarfs, ed. G. Wegner (New York: Springer), 156
Barstow, M. A., et al. 1993a, MNRAS, 264, 16
Barstow, M. A., Fleming, T. A., Finley, D. S., Koester, D., & Diamond, C. J. 1993b, MNRAS, 260, 631
Barstow, M. A., Hodgkin, S. T., Pye, J. P., King, A. R., Fleming, T. A., Holberg, J. B., & Tweedy, R. W. 1993c, in White Dwarfs: Advances in Observation and Theory, ed. M. A. Barstow (Dordrecht: Kluwer), 433
Bergeron, P. 1993, in White Dwarfs: Advances in Observation and Theory, ed. M. A. Barstow (Dordrecht: Kluwer), 267
Bergeron, P., Saffer, R. A., & Liebert, J. 1992, ApJ, 394, 228 (BSL)
Bergeron, P., Wesemael, F., & Fontaine, G. 1991, ApJ, 367, 253
Bergeron, P., Wesemael, F., Lamontagne, R., & Chayer, P. 1993, ApJ, 407, L85
Bohlin, R. C., & Grillmair, C. J. 1988, ApJS, 68, 487
Cassatella, A., Lloyd, C., & Gonzalez Riestra, R. 1987, IUE NASA Newsletter, No. 35, 225
Cheselka, M., Holberg, J. B., Watkins, R., Collins, J., & Tweedy, R. W. 1993, AJ, 106, 2365
Chayer, P., Pelletier, C., Fontaine, G., & Wesemael, F. 1993, in White Dwarfs: Advances in Observation and Theory, ed. M. A. Barstow (Dordrecht: Kluwer), 261
Dimitrijevic, M. S., & Sahal-Bréchot, S. 1984a, A&A, 136, 289
———. 1984b, J. Quant. Spectrosc. Rad. Transf., 31, 301
Dorman, B., Rood, R. T., & O'Connell, W. O. 1993, ApJ, 419, 596
Dreizler, S., & Werner, K. 1993, A&A, 278, 199
Drilling, J. S. 1992, in Lecture Notes in Physics, 401, The Atmospheres of Early-Type Stars, ed. U. Heber & S. Jefferey (New York: Springer), 257
Drilling, J. S., & Schönberner, D. 1985, A&A, 146, L23
Fich, M., & Blitz, L. 1984, ApJ, 279, 125
Finley, D. S., Basri, G., & Bowyer, S. 1990, ApJ, 359, 483
Finley, D. S., Jelinski, P., Dupuis, J., & Koester, D. 1993, ApJ, 417, 259
Finley, D. S. Koester, D., & Basri, G. 1994, in preparation
Fontaine, G., & Wesemael, F. 1987, in IAU Colloq. 95, The Second Conference on Faint Blue Stars, ed. A. G. Davis Philip, D. S. Hayes, & J. Liebert (Schenectady, NY: Davis), 319
Fulbright, M. S., Liebert, J., Bergeron, P., & Green, R. F. 1993, ApJ, 406, 240
Green, R. F., Schmidt, M., & Liebert, J. 1986, ApJS, 61, 305
Greenstein, J. L., & Sargent, A. 1974, ApJS, 28, 157
Harrington, R. S., & Dahn, C. C. 1980, AJ, 85, 454
Heber, U. 1986, A&A, 155, 33
Holberg, J. B. 1987, in IAU Colloq. 95, The Second Conference on Faint Blue Stars, ed. A. G. Davis Philips, D. S. Hayes, & J. Liebert (Schenectady, NY: Davis), 285
Holberg, J. B., Kidder, K., Liebert, J., & Wesemael, F. 1989, in IAU Colloq. 114, White Dwarfs, ed. G. Wegner (New York: Springer), 188
Holberg, J. B., Kidder, K. M., & Wesemael, F. 1990, ApJ, 365, L77
Jordan, S., Heber, U., Engels, D., & Koester, D. 1993, A&A, 273, L27
Jordan, S., Heber, U., & Weidemann, V. 1991, in 7th European Workshop on White Dwarfs, ed. G. Vauclair & E. M. Sion (Dordrecht: Kluwer), 121
Jordan, S., & Koester, D. 1986, A&AS, 65, 367
Kidder, K. 1991, Ph. D. thesis, Univ. Arizona
Kidder, K. M., Holberg, J. B., Barstow, M. A., Tweedy, R. W., & Wesemael, F. 1992, ApJ, 394, 288
Koester, D. 1989, ApJ, 342, 999
Koester, D., Liebert, J., & Saffer, R. A. 1994, ApJ, 422, 783
Koester, D., & Schönberner, D. 1986, A&A, 154, 125
Lamontagne, R., Wesemael, F., Bergeron, P., Liebert, J., Fulbright, M. S., & Green, R. F. 1993, in White Dwarfs: Advances in Observation and Theory, ed. M. A. Barstow (Dordrecht: Kluwer), 347
Liebert, J., Bergeron, P., & Tweedy, R. W. 1994, ApJ, 424, 817
Liebert, J., Green, R., Bond, H. E., Holberg, J. B., Wesemael, F., Fleming, T. A., & Kidder, K. 1989, ApJ, 346, 251
McCook, G. P., & Sion, E. M. 1987, ApJS, 65, 603
MacDonald, J., & Vennes, S. 1991, ApJ, 371, 719
Malina, R. F., et al. 1994, AJ, 107, 751
Margon, B., Liebert, J., Gatewood, G., Lampton, M., Spinrad, H., & Bowyer, S. 1976, ApJ, 209, 525
Michaud, G., Bergeron, P., Heber, U., & Wesemael, F. 1989, ApJ, 338, 417
Napiwotzki, R. 1992, in Lecture Notes in Physics, 401, The Atmospheres of Early-Type Stars, ed. U. Heber & S. Jefferey (New York: Springer), 310
Napiwotzki, R. 1993, Acta Astron., in press
Napiwotzki, R., Barstow, M. A., Fleming, T. A., Holweger, H., Jordan, S., & Werner, K. 1993, A&A, 278, 478
Napiwotzki, R., & Rauch, T. 1994, A&A, in press
Napiwotzki, R., & Schönberner, D. 1991, in 7th European Workshop on White Dwarfs, ed. G. Vauclair & E. M. Sion (Dordrecht: Kluwer), 39

Napiwotzki, R., & Schönberner, D. 1993a, in IAU Symp. 155, Planetary Nebulae, ed. R. Weinberger & A. Acker (Dordrecht: Kluwer), 495
———. 1993b, in White Dwarfs: Advances in Observation and Theory, ed. M. A. Barstow (Dordrecht: Kluwer), 99
Pounds, K. A., et al. 1993, MNRAS, 260, 77
Reid, I. N., & Wegner, G. 1988, ApJ, 335, 953
Saffer, R. A. 1991, Ph.D. thesis, Univ. Arizona
Schönberner, D. 1983, ApJ, 272, 708
Schöning, T., & Butler, K. 1989, A&AS, 78, 51
Seaton, M. J., Zeippen, C. J., Tully, J. A., Prandham, A. K., Mendoza, C., Hibbert, A., & Berrington, K. A. 1992, Rev. Mexicana Astron. Af., 23, 19
Shamey, L. 1969, Ph.D. thesis, Univ. Colorado
Shipman, H. L. 1976, ApJ, 206, L67
Szathmary, K. 1972, JRASC, 66, 219
Teays, T. J., & Garhart, M. P. 1990, IUE NASA Newsletter, No. 41, 94
Tweedy, R. W., Holberg, J. B., Barstow, M. A., Bergeron, P., Grauer, A. D., Liebert, J., & Fleming, T. A. 1993, AJ, 105, 1938
Tweedy, R. W., & Napiwotzki, R. 1992, MNRAS, 259, 315
Tweedy, R. W., et al. 1994, in preparation
van Altena, W. F., Lee, J. T., & Hoffleit, D. 1993, Yale General Catalogue of Trigonometric Stellar Parallaxes (New Haven, CT: Yale Univ. Press)
Vennes, S. 1992, ApJ, 490, 590
Vennes, S., Chayer, P., Fontaine, G., & Wesemael, F. 1989, ApJ, 336, L25
Vennes, S., & Fontaine, G. 1992, ApJ, 401, 288
Vennes, S., Pelletier, C., Fontaine, G., & Wesemael, F. 1988, ApJ, 331, 876
Vennes, S., Shipman, H. L., & Petre, R. 1990, ApJ, 364, 647
Vennes, S., Thjell, P., & Shipman, H. L. 1991, in 7th European Workshop on White Dwarfs, ed. G. Vauclair & E. M. Sion (Dordrecht: Kluwer), 235
Werner, K., & Dreizler, S. 1993, Acta Astron., in press
Wesemael, F., Auer, L. H., Van Horn, H. M., & Savedoff, M. P. 1980, ApJS, 43, 159
Wesemael, F., et al. 1994, ApJ, 429, 369
Wesemael, F., Green, R. F., & Liebert, J. 1985, ApJS, 58, 379
Wesemael, F., Greenstein, J. L., Liebert, J., Lamontagne, R., Fontaine, G., Bergeron, P., & Glaspey, J. W. 1993, PASP, 105, 761
Wood, M. A. 1990, Ph.D. thesis, Univ. Texas at Austin
Wood, M. A. 1994, in IAU Colloq. 47, The Equation of State in Astrophysics, ed. G. Chabrier (Cambridge: Cambridge Univ. Press), in press
Wood, M. A., & Bergeron, P. 1994, in preparation

Note added in proof.—A recent spectroscopic analysis of PG 0948 + 534 (classified sd in the PG catalog) indicates that this star is a hot DA white dwarf with $T_{\rm eff}$ = 130,000 K and log g = 7.4 assuming a pure hydrogen composition; the object is consistent with post-AGB evolution ($M > 0.6\ M_{\odot}$; see Fig. 13). The optical spectrum, kindly provided by R. A. Saffer, does not reveal any He II λ4686 feature. More interesting, the line profile fits exhibit the Balmer-line problem at a strong level, a result which rules out the presence of helium as the origin of the Balmer-line problem. PG 0948 + 534 thus represents the first DA star in which this problem has been reported. We note also that PG 0948 + 534 has not been detected in the *EUVE* and *ROSAT* surveys.